Search for the electroweak production of $Z\gamma$ pairs and measurement of the differential cross section of the $Z\gamma$ production in association with two jets with the ATLAS experiment at LHC.

PhD defense

Olympia Dartsi

supervised by Lucia Di Ciaccio

3 October 2019

ATLAS EXPERIMENT
http://atlas.ch

Enigmass

LAPP
Laboratoire d'Annecy-le-Vieux de Physique des Particules

Outline

The Standard Model of particle physics

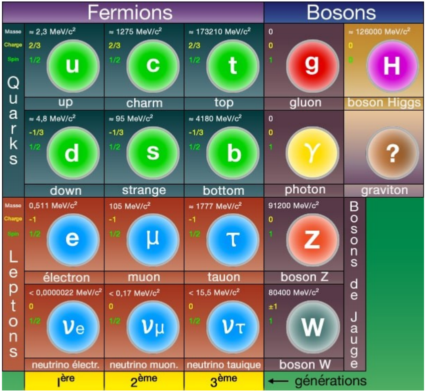

Standard Model (SM):

- Provides a unified picture of the fundamental particles and their interactions.
- Categorization into fermions and bosons.
- 3 kinds of interactions:
  - electromagnetic (γ)
  - weak ($W^{\pm}, Z$)
  - strong (g)
- Higgs $\rightarrow$ allowing the introduction of mass.

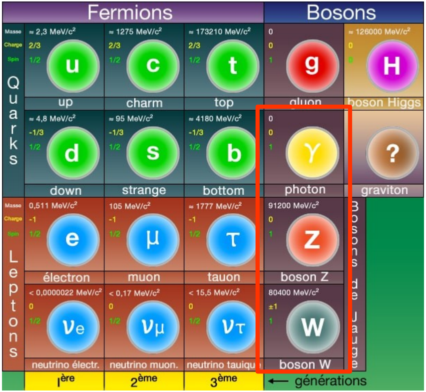

- The SM predicts interactions between the EW gauge bosons called self-interactions.

Standard Model (SM):

- Provides a unified picture of the fundamental particles and their interactions.
- Categorization into fermions and bosons.
- 3 kinds of interactions:
  - electromagnetic (γ)
  - weak ($W^{\pm}, Z$)
  - strong (g)
- Higgs $\rightarrow$ allowing the introduction of mass.

The Standard Model of particle physics

Triple & quartic gauge couplings are central predictions of the EW theory

$$\mathcal{L}_{kin} = -\frac{1}{4} W^i_{\mu\nu} W_i^{\mu\nu} =$$

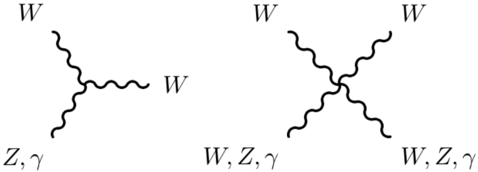

- no neutral gauge boson self-couplings in the SM (at tree level)

Gauge boson self-interactions are responsible for vector boson scattering.

VBS $\Rightarrow$ rare processes ($VV \rightarrow VV$, $V = W^{\pm}, Z, \gamma$)
$\Rightarrow$ probe the non-Abelian structure of the EW interactions

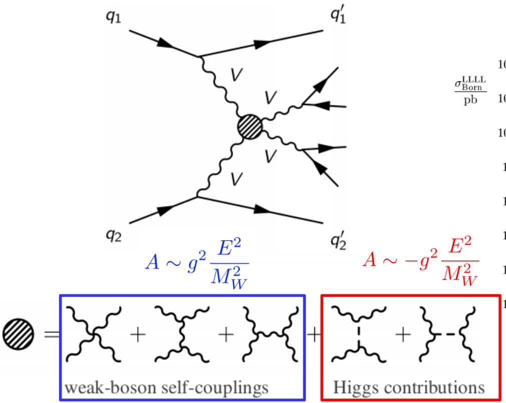

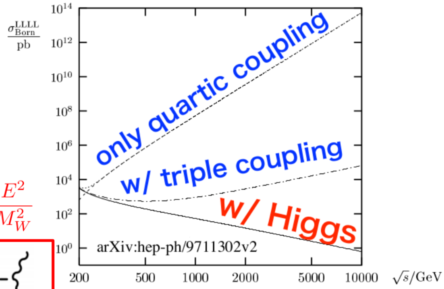

- Higgs boson restores unitarity of the scattering amplitude.

$\Rightarrow$ the study of high-energy behaviours of VBS is crucial to understand the nature of EWSB in the SM

Vector Boson Scattering beyond the Standard Model

New physics could modify couplings between bosons leading to anomalous triple and anomalous quartic gauge couplings

- presence of aGCs enhances EW cross-section and it's more pronounced at high-energy tails (m_{VV}, E_T, p_T).
  - $\Rightarrow$ examine variables that carry the energy of the system: p_T or mass

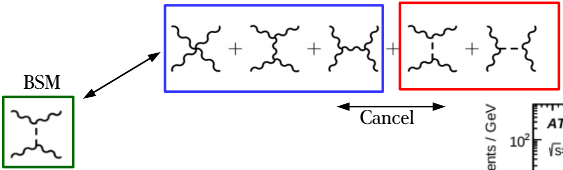

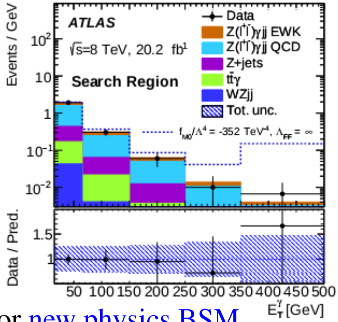

- Heavy resonances ($m > \mathcal{O}(5)$ TeV)
- $Z\gamma jj \rightarrow$ in SM no TGC and one QGC ($WWZ\gamma$)

Any deviation from the SM predictions $\rightarrow$ a hint for new physics BSM.

Vector Boson Scattering - diagram

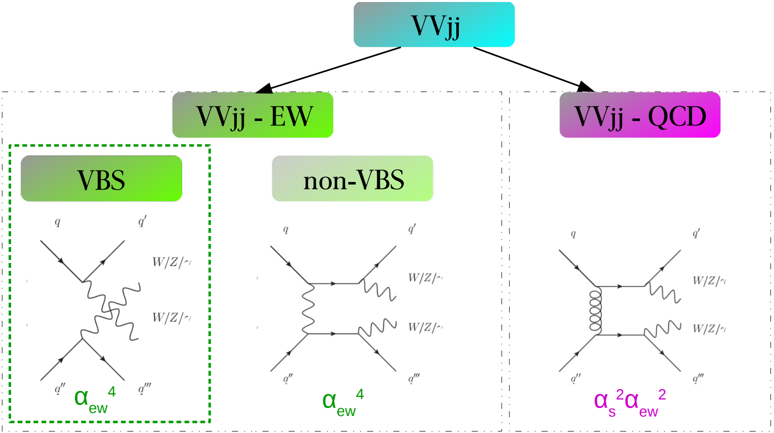

VVjj processes ⇒ produced through a combination of strong (QCD) and EW interactions.

- *VVjj*-EW (VBS and non-VBS), can not be separated ⇒ signal
- *VVjj*-QCD ⇒ background

Vector Boson Scattering - diagram

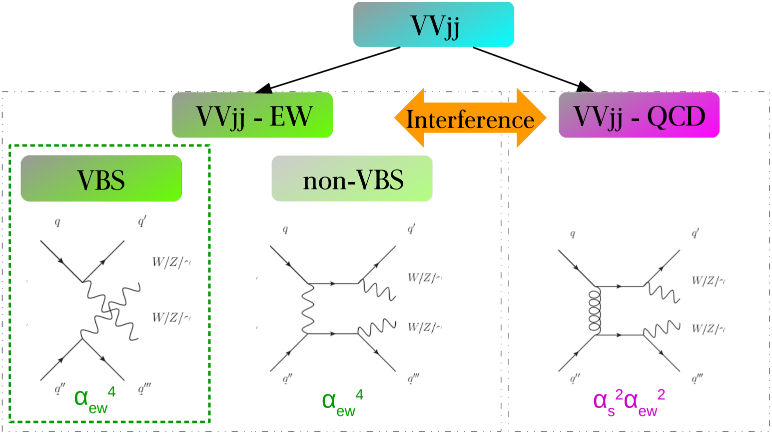

- Interference occurs between *VVjj*-EW & *VVjj*-QCD production.

Vector Boson Scattering - event topology

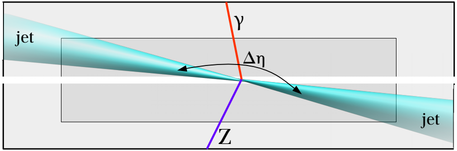

- Vector bosons → centrally with respect to the jets

- Two hadronic jets in forward and backward regions (**tagging jets**) with very high energy & high invariant mass

- hadronic activity suppressed between the two jets (**rapidity gap**)

$$\zeta(Z\gamma) = \left| \frac{y_{Z\gamma} - (y_{j1} + y_{j2})/2}{\Delta Y_{jj}} \right|$$

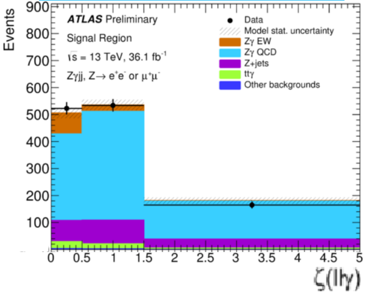

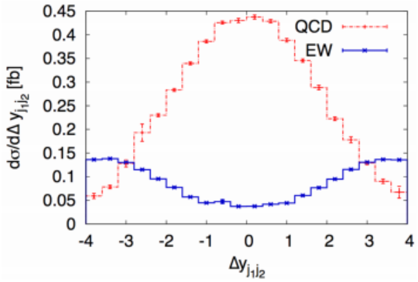

Status of the *VVjj*-EW search in pp collisions

VVjj-EW	ZZ	$Z\gamma$	$\gamma\gamma$	WZ	W^+W^-	$W^\pm W^\pm$	$W\gamma$

■ observed, ■ evidence

ATLAS-CONF-2019-033

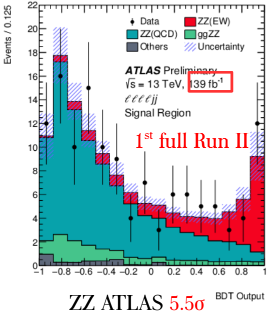

ZZ ATLAS 5.5σ

CMS-PAS-SMP-18-007

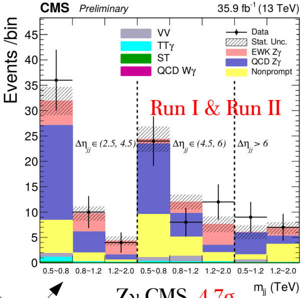

Zγ CMS 4.7σ

EPS-HEP July 2019

ATLAS-CONF-2019-033

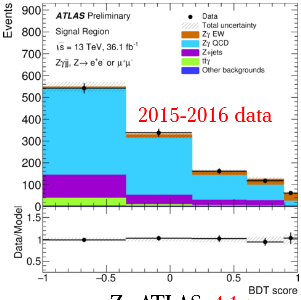

Zγ ATLAS 4.1σ

LP Aug. 2019

$Z\gamma jj$-EW production - Motivation

- So far the $Z\gamma jj$-EW production has never been observed.
- Observation is expected with full RunII data.

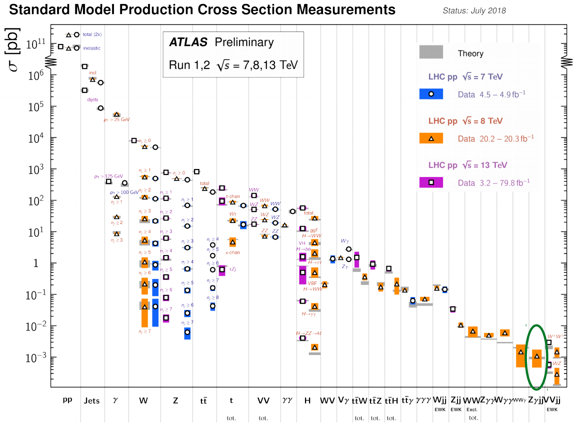

- **Aim**:

  observe & measure EW cross-section
- **Experimental challenge**:

  EW → two orders of magnitude lower than QCD.

The Large Hadron Collider

The Large Hadron Collider

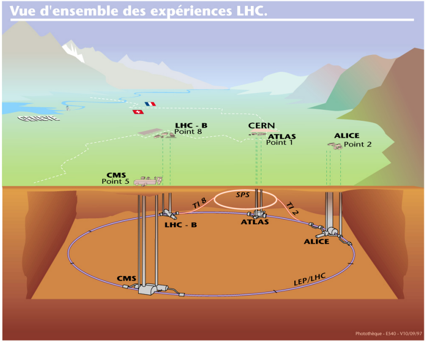

- World's largest particle collider.
- Hadron-hadron accelerator.
- Accelerator parameters:

$$N = \mathcal{L} \times \sigma$$

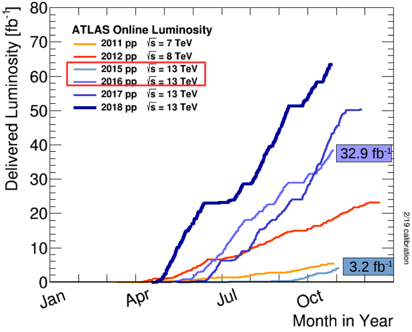

- $\sqrt{s} = 13$ TeV
- In 2015-2016 data $\mathcal{L} = 36.1$ fb^{-1}
- RunII full stat. $\mathcal{L} = 139$ fb^{-1}

The ATLAS Detector

One of the two general-purpose detectors with forward-backward symmetry.

- ATLAS trigger system preselects events which may be of interest
- Purpose: to record information about the final state particles

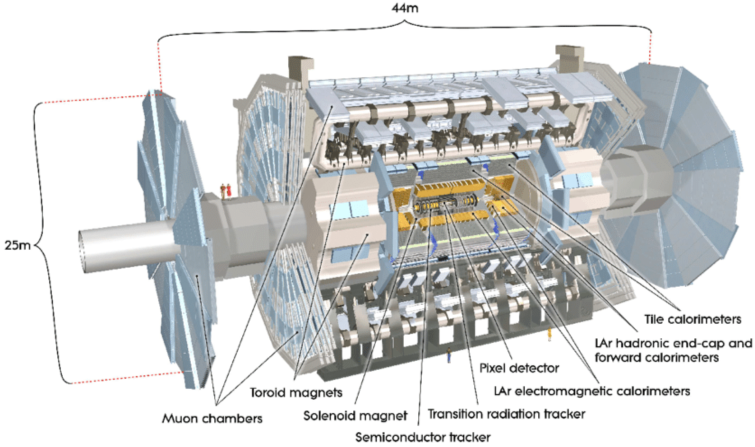

The ATLAS Detector

- **Calorimeters**
  - → electromagnetic: electrons & photons
  - → hadronic: hadrons
- **Inner Detector**
  - → reconstruct charged particle tracks
  - → solenoid magnetic field 2 T

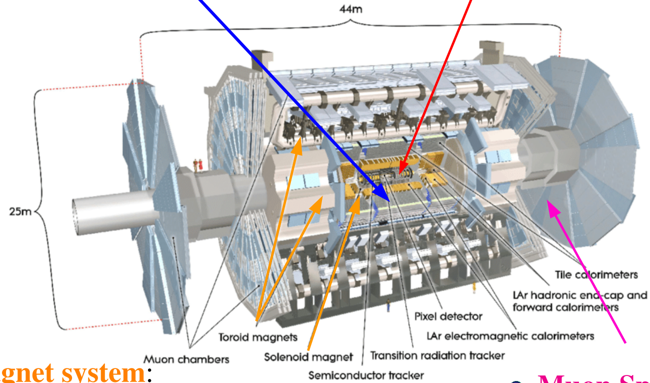

- **Magnet system**: curves the trajectory of charged particles
- **Muon Spectrometer**
  - → reconstruct muons
  - → toroid magnetic field

In RunII a new ID layer (IBL) is introduced.

Electron Performance Studies

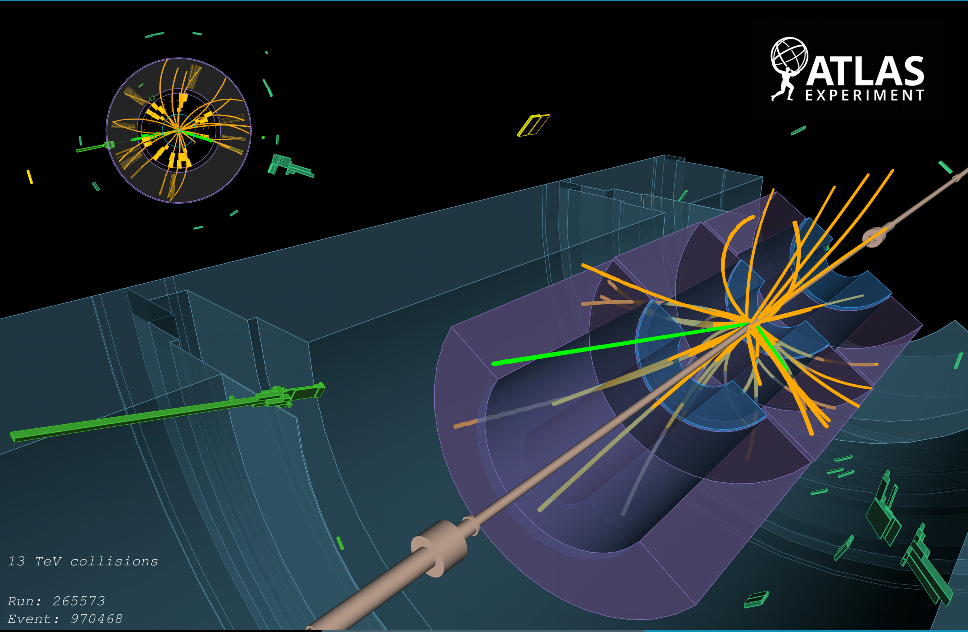

Electron Identification

Electron identification play a crucial role in the $Z\gamma jj$ analysis.

Electron identification: track (ID) + energy deposit (ECAL).

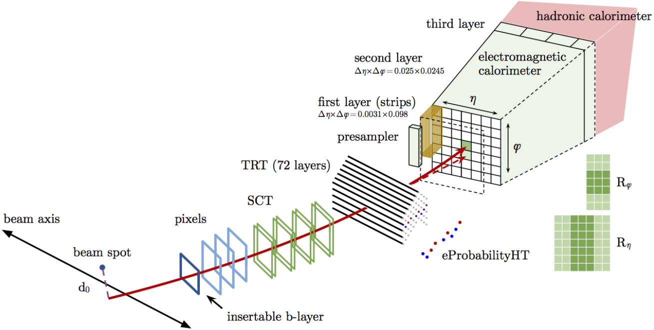

A Likelihood method algorithm is built from:

- track variables (number of hits, d_0, ...)
- calorimeter shower shapes variables
- track-cluster matching ($\Delta\eta$, $\Delta\phi$)

3 identification menus of signal efficiency with respect to the background rejection:

- *Loose*, *Medium* & *Tight*

Electron identification efficiency methodology

Measure the identification efficiency in data.

Tag-and-probe method of $Z \to ee$:

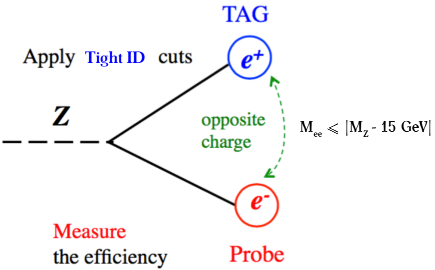

$E_T > 15$ GeV

$$\epsilon_{\text{ID}}^{\text{Data}} = \frac{N_{\text{pass ID}} - N_{\text{pass ID}}^{\text{BKG}}}{N_{\text{pass ID}} + N_{\text{fail ID}} - (N_{\text{pass ID}}^{\text{BKG}} + N_{\text{fail ID}}^{\text{BKG}})}$$

Verify that the ϵ_{ID} is well modeled in MC $\to$ correction factor from data.

$$SF = \frac{\epsilon_{\text{ID}}^{\text{Data}}}{\epsilon_{\text{ID}}^{\text{MC}}}$$

$Z \rightarrow ee$ background evaluation

Zmass Method

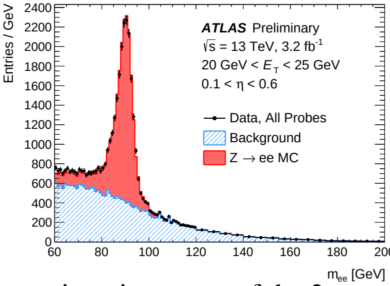

- invariant mass of the 2 electrons $\sim$ Z-boson mass.
- uses sidebands to constrain the background.

$\rightarrow$ In bins of η and E_T (15-150 GeV)

I contributed to the Z_{iso} method.

ZIso Method

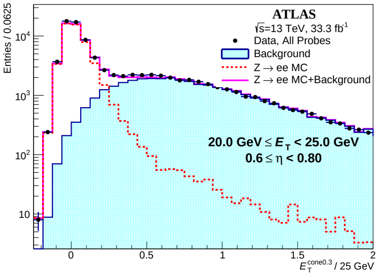

- electrons produced from the $Z \rightarrow ee$ decay are isolated.
- uses the probe isolation to constrain the background.

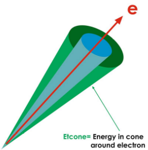

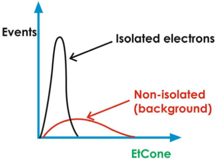

Comparison between Zmass and ZIso results

- At low E_T bin discrepancy on SFs between Z_{iso} & Z_{mass} method.
- Fair agreement is found in the higher E_T bins.

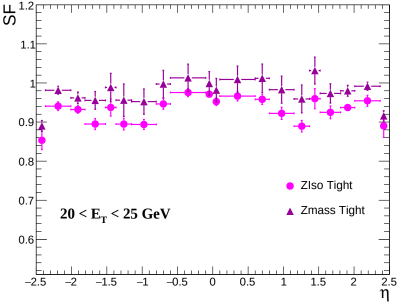

- The main impact (up to 5%) was found related to the modeling of the shape of the data driven background

Tag-and-probe method of $Z \to ee\gamma$:

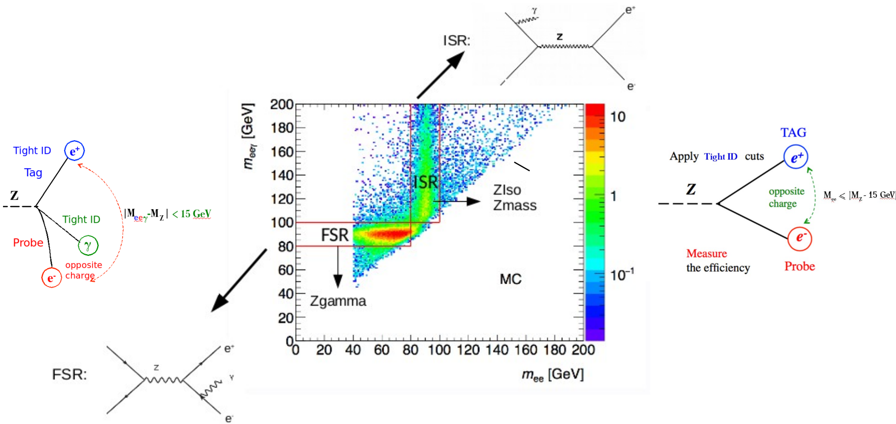

$E_T > 10$ GeV

- understanding of the discrepancy between Zmass and Ziso
- extended the E_T range of Z methods in the 10-15 GeV bin

Electron identification efficiency with $Z \to ee\gamma$ events

- Less background probes than the $Z \to ee$ methods.

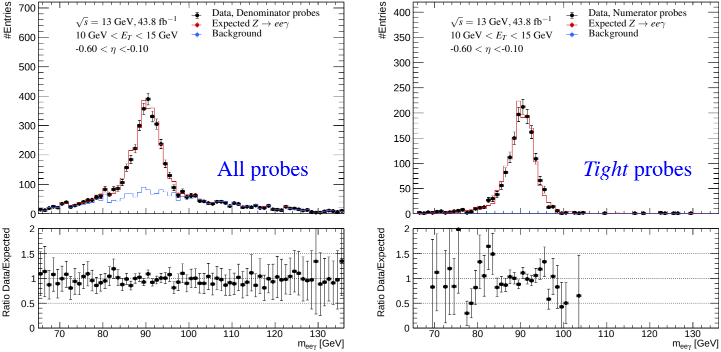

- invariant mass of the 3 objects ∼ Z-boson mass
- uses sidebands to constrain the background as Zmass method

I developed & implemented this method in the ATLAS software.

Electron SFs with $Z \to ee$ & $Z \to ee\gamma$ methods

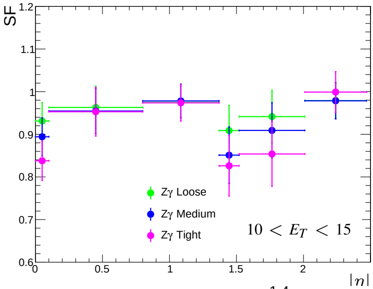

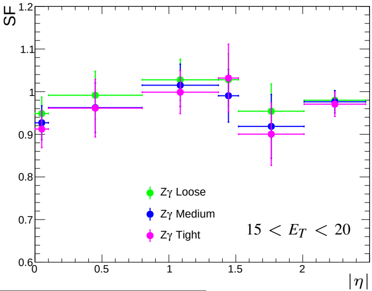

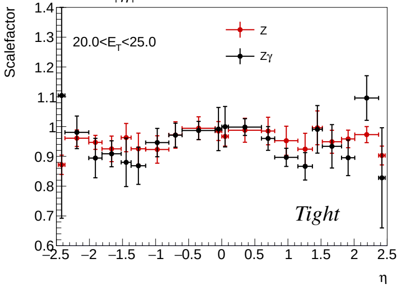

Combined SFs

- 7-10 GeV: $J/\psi \to ee$ method,
- 10-15 GeV: $J/\psi \to ee$ and $Z \to ee\gamma$ methods combined,
- 15-20 GeV: all methods combined,
- above 20 GeV: $Z \to ee$ method.

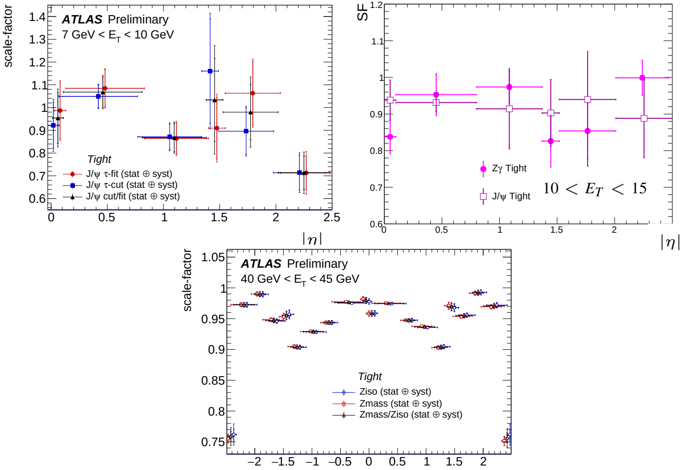

$Z\gamma jj$ analysis

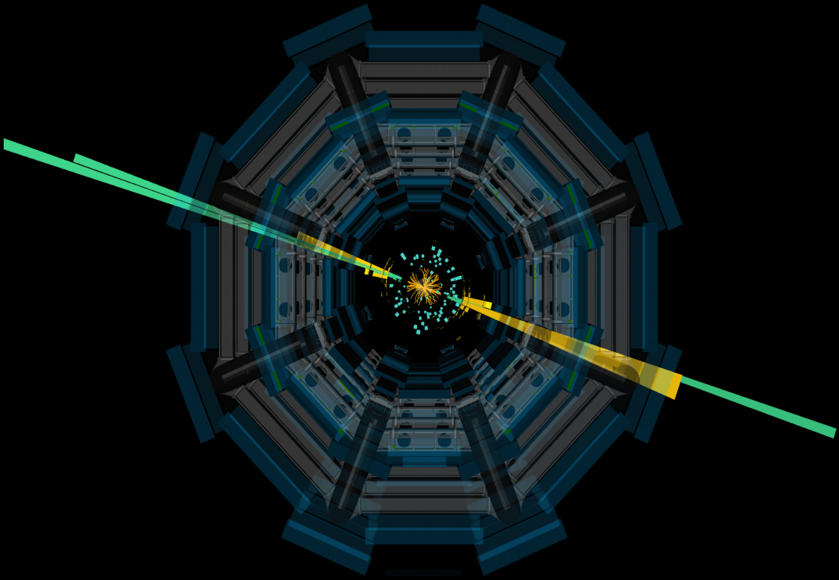

1. Event selection
2. Control regions and background estimation
3. Interference studies
4. Results from the fit:
   - signal strength & integrated cross-section measurement
   - differential cross-section measurement

$Z\gamma jj$ event selection

Signal object selection:

- ≥ 2 jets $p_T > 30$ GeV
- $= 2$ leptons $p_T > 20$ GeV & isolated
- ≥ 1 photon $E_T > 15$ GeV & isolated

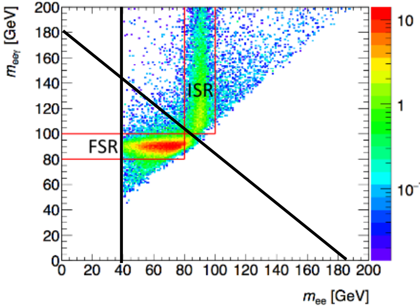

Boson mass	$m_{\ell^+\ell^-} > 40$ GeV $m_{\ell^+\ell^-} + m_{\ell^+\ell^-\gamma} > 182$ GeV
VBS baseline selection	$p_T > 50$ GeV of two tagging jets $\lvert\eta\rvert < 4.5$ of two tagging jets $m_{jj} > 150$ GeV $\zeta(Z\gamma) < 5$ $\lvert\Delta\eta_{jj}\rvert > 1$

$$m_{jj} = \sqrt{((E_{j1} + E_{j2})^2 - (\vec{p}_{j1} + \vec{p}_{j2})^2)}$$

$$\zeta(Z\gamma) = \left| \frac{y_{Z\gamma} - (y_{j1} + y_{j2})/2}{\Delta Y_{jj}} \right|$$

Irreducible background ($\rightarrow$ 2 prompt leptons and a prompt photon):

- $Z\gamma jj$-QCD $\rightarrow$ m_{jj} smaller than $Z\gamma jj$-EW
- $t\bar{t}\gamma$ $\rightarrow$ has b-jets

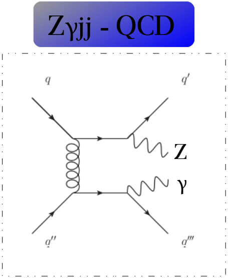

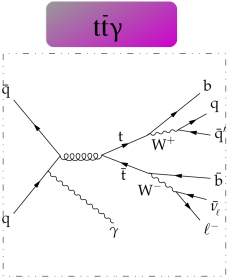

How to evaluate the remaining irreducible background?

- exploit the m_{jj} shape in a MVA
- use a control region with no b-jets

Reducible background ($\rightarrow$ mis-identified jet as γ or ℓ):

- Z+jets $\rightarrow$ fake-photon
- WZ, single top $\rightarrow$ small contributions $\rightarrow$ estimated using MC

Z+jets

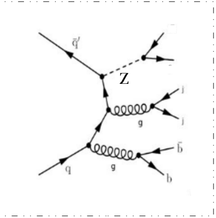

WZ

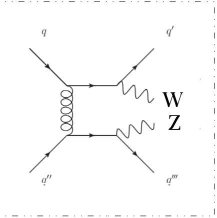

Single top

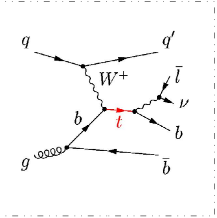

How to evaluate the remaining reducible background?

- apply photon isolation
- require tight photon

Discrimination signal from background methodology

- baseline method⇒ BDT approach ($p_T(Z\gamma), \zeta(Z\gamma), m_{Z\gamma}, m_{jj}$)
- cross-check method⇒ cut-based approach ($\zeta(Z\gamma)$)

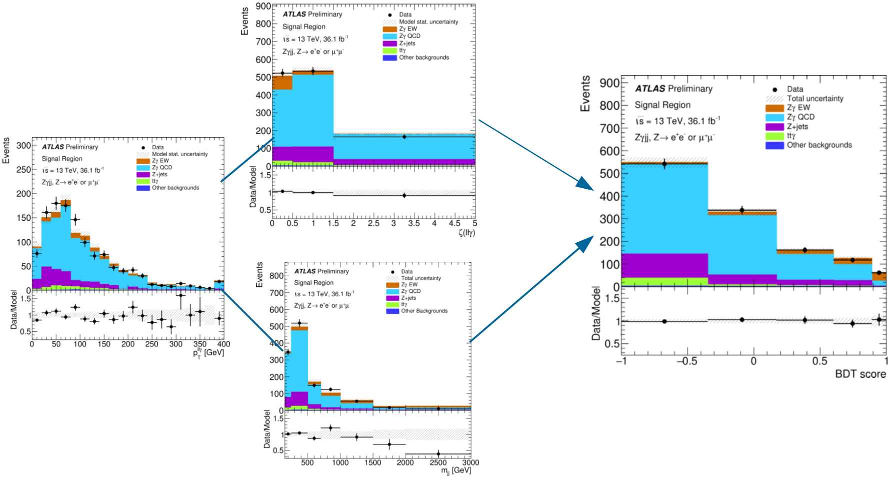

Analysis regions

The phase space divided into:

2 regions for **BDT approach**:

BDT-R : rich in $Z\gamma jj$-EW & QCD

b-CR: rich in $t\bar{t}\gamma$

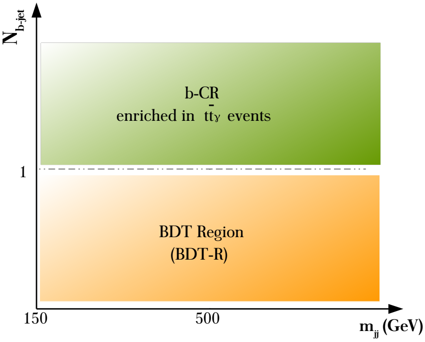

3 regions for **cut-based approach**:

SR : rich in $Z\gamma jj$-EW

QCD-CR : rich in $Z\gamma jj$-QCD

b-CR: rich in $t\bar{t}\gamma$

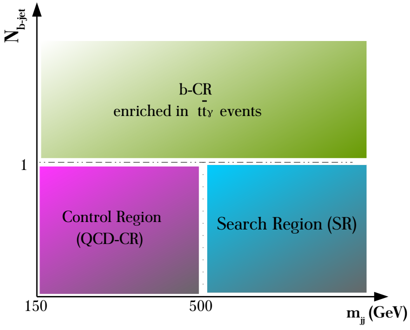

Background estimation & event yield

Z+jets$\Rightarrow$ a 2D sideband data-driven (ABCD) method is used (15%)

$Z\gamma jj$-QCD$\Rightarrow$ normalization factor estimated with the ABCD method and then obtained from the fit (73%)

$t\bar{t}\gamma\Rightarrow$ a dedicated control region is built, b-CR (3%)

WZ and single top$\Rightarrow$ are estimated by MC (0.5%)

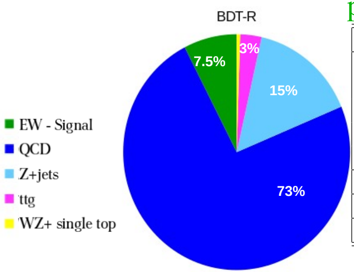

prefit

	SR	QCD-CR	b-CR	BDT-R
$Z\gamma jj$-QCD	268 ± 16	745 ± 25	96 ± 10	1013 ± 30
Z+jets	56 ± 3	156 ± 6	20 ± 4	213 ± 7
$t\bar{t}\gamma$	$13 \pm 1.$	35 ± 2	264 ± 4	48 ± 2
$WZjj$	1.7 ± 0.1	2.7 ± 0.2	0.3 ± 0.0	4.4 ± 0.2
Single top	1.0 ± 0.5	1.3 ± 0.4	4.0 ± 0.8	2.3 ± 0.7
$Z\gamma jj$-EW (signal)	76 ± 1	28 ± 1	4.8 ± 0.2	104 ± 1
Total MC	415 ± 16	968 ± 26	389 ± 10	1384 ± 31
Data	356	866	388	1222

Simulations: $Z\gamma jj$-QCD$\Rightarrow$ SHERPA V.2.2.2 @ NLO
$Z\gamma jj$-EW$\Rightarrow$ MADGRAPH5 @ LO

Interference of strong and electroweak production

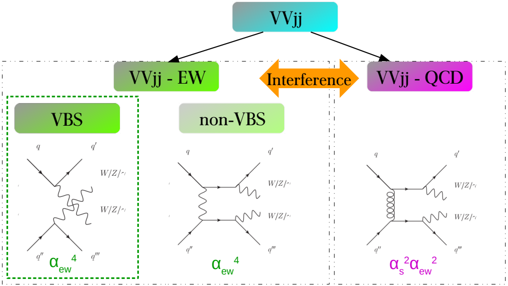

VVjj-EW & *VVjj*-QCD: identical initial and final state ⇒ interfere with each other

- In the **RunI** the interference effect was small compared to the statistical uncertainty.
- In **RunII** using MC simulations we revisited the interference effect.

Interference of strong and electroweak production

There are two ways to evaluate the size of the EW-QCD interference term on the total $Z\gamma jj$ cross section:

- **Indirect way**$\Rightarrow$ calculating $\sigma_{EW}, \sigma_{QCD}$ and σ_{EW+QCD}
- **Direct way**$\Rightarrow$ calculating interference term using MadGraph

The cross section of the process is proportional to:

$$|M|^2 = |M_1 + M_2|^2 = |M_1|^2 + |M_2|^2 + 2 \times Re(M_2^* \times M_1)$$

- ◇ Zγjj-EW: $|M_1|^2 \propto (\mathcal{O}(\alpha_w^4))$
- ◇ Zγjj-QCD: $|M_2|^2 \propto (\mathcal{O}(\alpha_s^2\alpha_w^2))$
- ◇ Interference: $2 \times Re(M_2^* \times M_1) \propto (\mathcal{O}(\alpha_s\alpha_w^3))$

In RunII the interference effect is estimated to be:

$$\textbf{SR} : (1.9 \pm 0.1)\%$$

$$\textbf{BDT-R} : (3.5 \pm 0.3)\%$$

Controlling the interference

Investigation of the optimization of the phase-space definition.

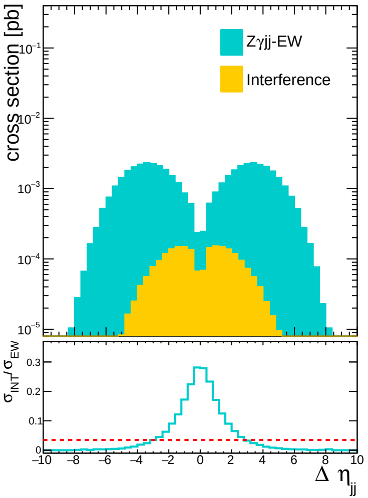

- $\Delta\eta_{jj}$ has the most discriminant power between the two contributions

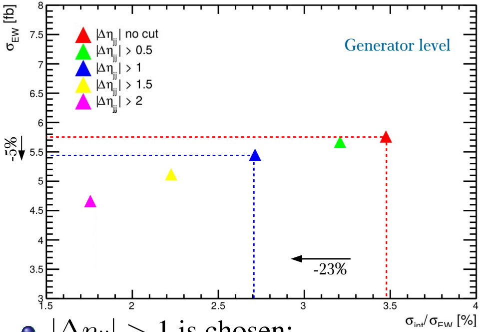

- $|\Delta\eta_{jj}| > 1$ is chosen:
  SR : $(1.6 \pm 0.1)\%$
  BDT-R : $(2.7 \pm 0.2)\%$

Treatment of the interference

The interference effect is not included in the $Z\gamma jj$-QCD measurement $\Rightarrow$ the observed cross section formally corresponds to the EW production including the interference effects.

The idea is:

- To assign the effect of the interference on the shape of the signal template as an uncertainty.

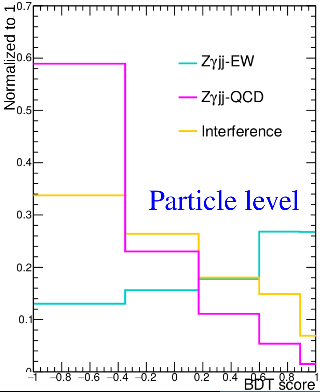

- Estimation of this uncertainty by adding the two distributions
- Interference uncertainty$\Rightarrow$ difference between EW and EW+Int

$$\text{weight} = \frac{EW + Int}{EW}$$

Treatment of the interference

The interference effect is not included in the $Z\gamma jj$-QCD measurement $\Rightarrow$ the observed cross section formally corresponds to the EW production including the interference effects.

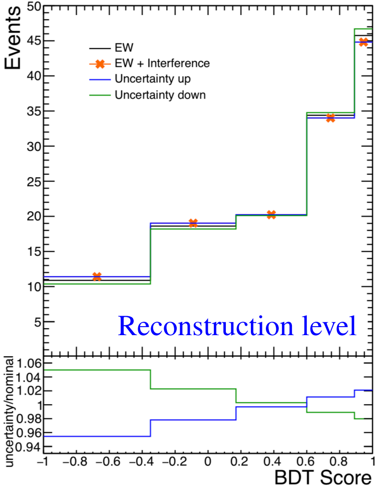

- Estimation of this uncertainty by adding the two distributions
- Interference uncertainty$\Rightarrow$ difference between EW and EW+Int

$$\text{weight} = \frac{EW + Int}{EW}$$

Fit procedure

Multivariate approach → gives as an output a BDT score distribution.

→ signal-like or background-like output

→ used in the fit to extract the signal strength

Signal strength:

$\mu_{\text{EW}} = N^{\text{EW}}_{\text{meas}} / N^{\text{EW}}_{\text{exp}}$

- binned likelihood fit
- expected results → using Asimov pseudo-data

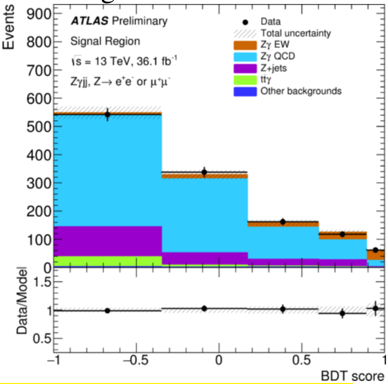

$\mu_{EW} = 1.00^{+0.19}_{-0.18}\,(\text{stat})^{+0.08}_{-0.10}\,(\text{MCstat})^{+0.09}_{-0.08}\,(\text{syst})^{+0.13}_{-0.10}\,(\text{theo})$

Observed significance 4.1σ

Fit procedure

Multivariate approach → gives as an output a BDT score distribution.

→ signal-like or background-like output

→ used in the fit to extract the signal strength

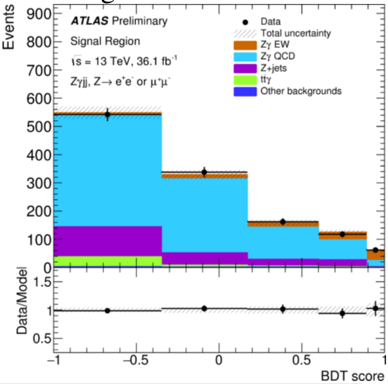

Signal strength:

$\mu_{\mathrm{EW}} = N^{\mathrm{EW}}_{\mathrm{meas}} / N^{\mathrm{EW}}_{\mathrm{exp}}$

- binned likelihood fit
- expected results → using Asimov pseudo-data

$$\mu_{EW} = 1.00 \,{}^{+0.19}_{-0.18}(\mathrm{stat}) \,{}^{+0.08}_{-0.10}\,(\mathrm{MCstat})\,{}^{+0.09}_{-0.08}\,(\mathrm{syst})\,{}^{+0.13}_{-0.10}\,(\mathrm{theo})$$

Observed significance 4.1σ

Cross-section measurements

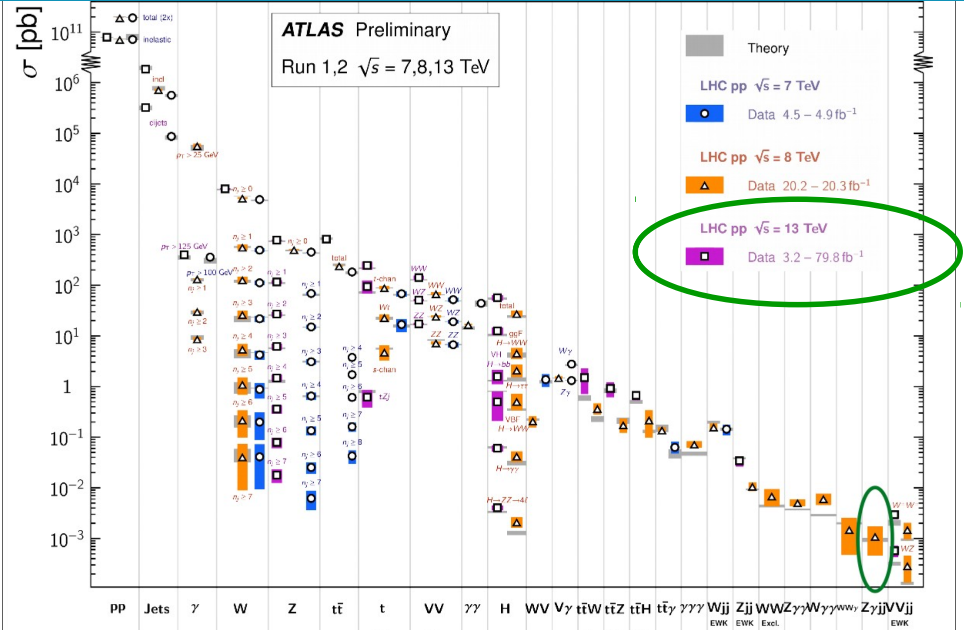

Integrated cross-section measurement

$$\sigma^{\text{fid.}}_{\text{obs. EW}} = 7.8 \boxed{{}^{+1.5}_{-1.4}\,(\text{stat.})}\ {}^{+0.9}_{-1.0}(\text{exp.syst}){}^{+1.0}_{-0.8}\,(\text{model.syst})\ \text{fb}$$

Source	Uncertainty [%]
Statistical	${}^{+19}_{-18}$
$Z\gamma jj$-EW theory modeling	${}^{+10}_{-6}$
$Z\gamma jj$-QCD theory modeling	± 6
$t\bar{t}\gamma$ theory modeling	± 2
$Z\gamma jj$-EW and $Z\gamma jj$-QCD interference	${}^{+3}_{-2}$
Jets	± 8
Pile-up	${}^{+6}_{-4}$
Electrons	± 1
Muons	${}^{+3}_{-2}$
Photons	± 1
Electrons/photons scale	± 1
b-tagging	± 2
MC statistics	± 8
Backgrounds normalization	${}^{+9}_{-8}$
Luminosity	± 2
Total Systematics	${}^{+27}_{-25}$

$$\sigma^{\text{fid.}}_{\text{exp. EW}} = 7.75 \pm 0.03(\text{stat}) \pm 0.2(\text{PDF} + \alpha_s) \pm 0.4(\text{scale})\ \text{fb}$$

$$\sigma^{\text{fid.}}_{\text{obs. }EW+QCD} = 71 \boxed{\pm 2\,(\text{stat.})}\ {}^{+9}_{-7}\,(\text{exp.syst}){}^{+21}_{-17}\,(\text{model.syst})\ \text{fb}$$

Differential cross-section measurements - motivation

Measurement by combined $Z\gamma jj$-QCD and $Z\gamma jj$-EW.

Interesting observables:

- P_T^γ, $M_{Z\gamma}$, M_{jj} $\Rightarrow$ sensitive in the high value tails to aQGCs
- N_{jets} $\Rightarrow$ to probe the QCD modeling

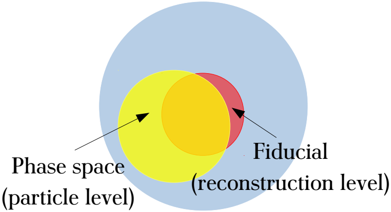

Extrapolation from detector to particle level:

- results can be compared to theory and other experiments

- Detector effects distort the distribution of the measured observables.
- The procedure of correcting these distortions is known as unfolding.

Differential cross-section measurements

$$\sigma_k = \frac{1}{L} \times \frac{1}{\epsilon_k} \times \sum_j M^{-1}_{jk} (N^{\text{obs}}_j - N^{\text{bkg}}_j) \times A_j$$

$$A_j = \frac{\mathrm{N}_j(reco\&gen)}{\mathrm{N}_j(reco)}$$

$$\epsilon_k = \frac{\mathrm{N}_k(reco\&gen)}{\mathrm{N}_k(gen)}$$

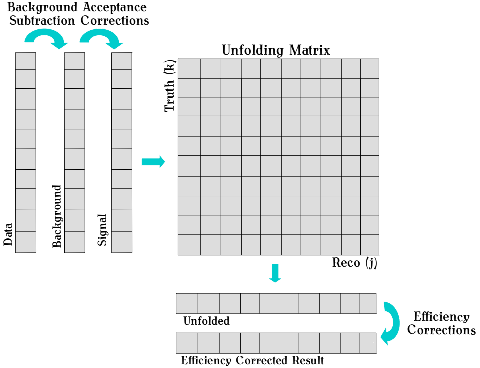

M_{jk} → probability for an event in bin k at **particle level** to end up in bin j at **reconstruction level**.

Differential cross-section measurements

A Bayesian iterative method is used:

- no inversion of the M_{jk}
- Bayes' theorem:

MC wanted

$$P(true|obs) = \frac{P(obs|true)f(true)}{g(obs)}$$

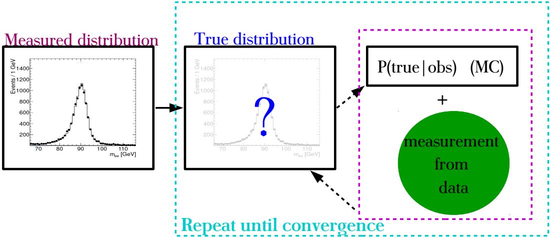

- estimation of the true spectra with an iterative procedure

$$f^{r+1}(true) = \int f^{r}(true)\frac{g(obs)_{data}}{g^{r}(obs)}P(true|obs)dobs$$

- more iterations:
  - ⇒ closer to the true distribution
  - ⇒ higher statistical uncertainty

- Measured in the SR of the cut-based approach.
- The binning of the observables is chosen depending on the statistics & resolution.
- Migration matrix → combining $Z\gamma jj$-EW & $Z\gamma jj$-QCD (MC).

Systematic uncertainties of the background

- *WZ* & single top ⇒ from MC (normalization & shape). [±20%]
- $t\bar{t}\gamma$ ⇒ shape from MC & normalization from b-CR. [±20%]
- *Z*+jets ⇒ normalization from the ABCD method [±20%]
  & shape from the $Z\gamma jj$-QCD MC sample [shape difference]

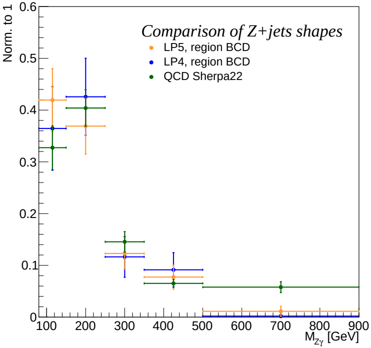

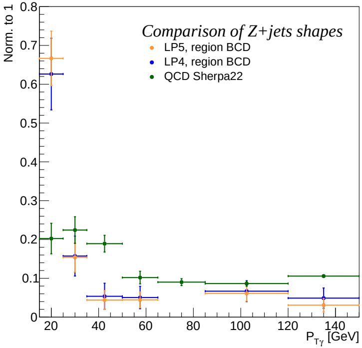

Other systematic uncertainties

- Objects used in the analysis: quadratic sum of each category
  - **leptons**: scale, resolution, efficiency and trigger.
  - **jets**: modeling, calibration, flavor, pile-up and efficiency.
  - **photons**: isolation and identification efficiency.
- Due to the unfolding method:

migration matrix	**Data to unfold**
SHERPA v2.2.2 $Z\gamma jj$-QCD and EW	data
SHERPA v2.1 $Z\gamma jj$-QCD and MADGRAPH $Z\gamma jj$-EW	data

Differential cross-section measurement - results: $M_{Z\gamma}$

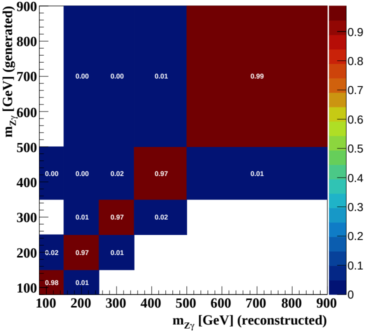

- the migration matrix is diagonal (2 iterations)
- purity: 75%-80%
- efficiency: 35%

$$\text{purity} = \left(\frac{\mathrm{N}(reco\&gen)}{\mathrm{N}(reco)} \right)_i \qquad \epsilon_k = \frac{\mathrm{N}_k(reco\&gen)}{\mathrm{N}_k(gen)}$$

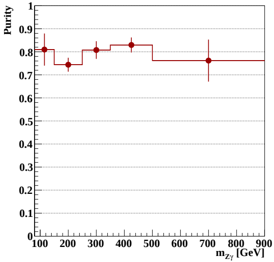

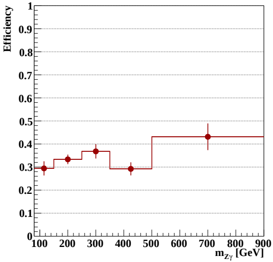

Differential cross-section measurement - results: $M_{Z\gamma}$

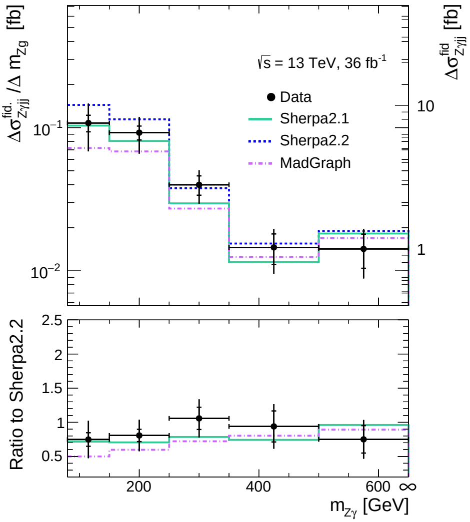

$m_{Z\gamma}$ [GeV]	80 – 150	150 – 250	250 – 350	350 – 500	$\geq$ 500
$\Delta\sigma^{\text{fid.}}_{Z\gamma jj}$ [fb]	7.55	9.23	3.99	2.19	1.00
Relative Uncertainties [%]					
Statistics	13.2	11.1	15.4	24.2	26.7
All systematics	34.2	26.4	21.5	25.0	26.8
Luminosity	2.8	2.6	2.5	2.6	2.3
Total	36.7	28.7	26.4	34.8	37.9
Uncorrelated syst.	1.0	1.2	1.4	1.7	1.3
Unfolding	0.9	0.4	0.7	1.1	0.5
Electrons	1.0	0.9	1.2	1.6	3.6
Muons	1.9	1.9	2.0	2.8	3.2
Photons	1.9	1.2	1.1	1.3	1.4
Jets	11.4	7.3	4.5	8.9	3.8
Z+jets Back.	29.0	24.3	18.3	19.7	21.9
Other Red. Back.	0.2	0.1	0.1	0.1	0.1
Irred. Background	1.0	1.2	1.4	1.7	1.3
Pileup	7.7	3.1	3.9	1.5	0.5

Predictions:

SHERPA2.2: EW & QCD SHERPA2.2

MADGRAPH: EW & QCD MADGRAPH

SHERPA2.1: EW SHERPA2.2 & QCD SHERPA2.1

Differential cross-section measurement - results: N_{jets}

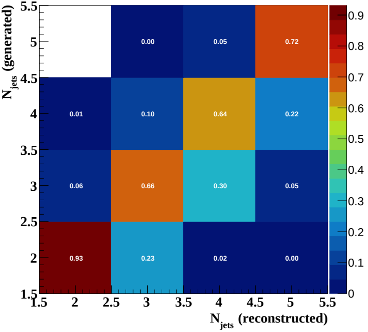

- the migration matrix is diagonal (3 iterations)
- purity: 60%
- efficiency: 32%

$$\text{purity} = \left(\frac{\text{N}(reco\&gen)}{\text{N}(reco)}\right)_i \qquad \epsilon_k = \frac{\text{N}_k(reco\&gen)}{\text{N}_k(gen)}$$

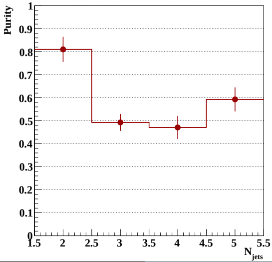

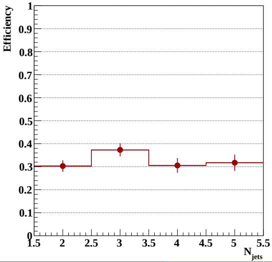

Differential cross-section measurement - results: N_{jets}

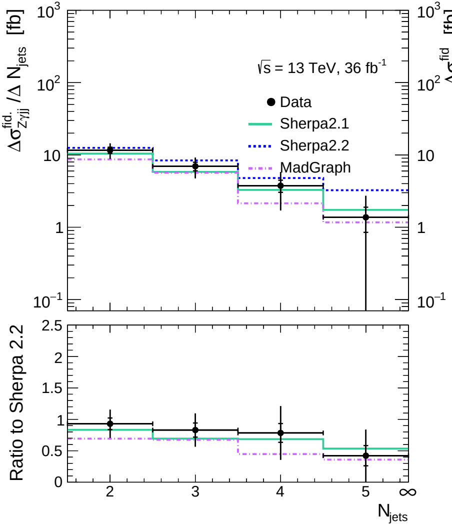

N_{jets}	$1-2$	$2-3$	$3-4$	≥ 4
$\Delta\sigma^{fid.}_{Z\gamma jj}$ [fb]	11.63	6.97	3.75	1.37
Relative Uncertainties [%]				
Statistics	9.9	13.5	19.1	38.0
All systematics	22.0	28.9	51.1	90.7
Luminosity	2.6	2.6	2.9	2.8
Total	24.1	31.9	54.5	98.3
Uncorrelated syst.	2.0	3.9	4.8	8.6
Unfolding	2.1	1.8	1.7	1.9
Electrons	0.8	0.8	0.9	0.8
Muons	1.9	2.0	1.7	2.9
Photons	1.2	1.6	1.8	1.3
Jets	9.2	7.7	35.0	66.7
Z+jets Back.	16.7	26.1	34.3	57.2
Other Red. Back.	0.1	0.2	0.1	0.3
Irred. Background	2.0	3.9	4.8	8.6
Pileup	5.0	3.3	5.4	9.6

Predictions:

SHERPA2.2: EW & QCD SHERPA2.2

MADGRAPH: EW & QCD MADGRAPH

SHERPA2.1: EW SHERPA2.2 & QCD SHERPA2.1

Differential cross-section measurement - results: P_T^{γ}, M_{jj}

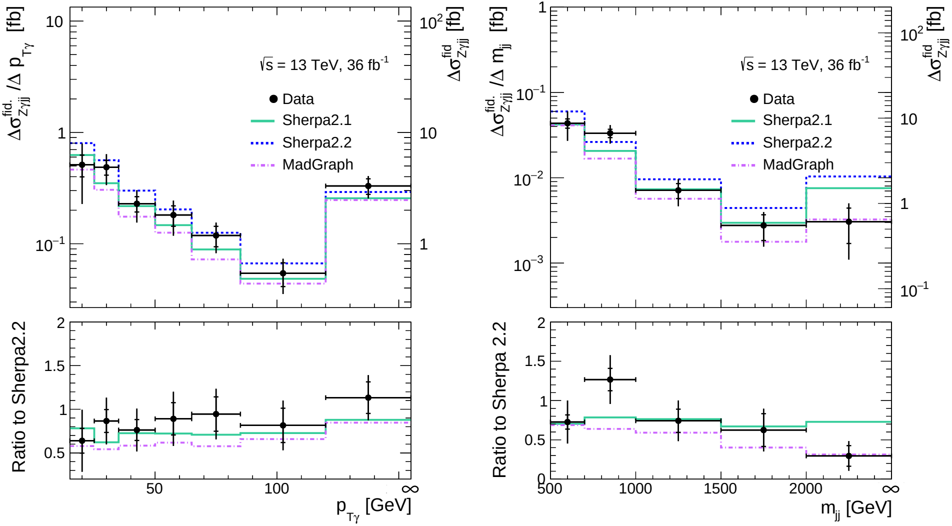

Summary & Outlook

- Measurement of electron ID efficiencies for the ATLAS
- Evidence of the $Z\gamma jj$-EW production reached:
  - the cross-section is in agreement with predictions
  - electron identification contribute with an uncertainty $\pm 1\%$
  - the interference effect between the $Z\gamma jj$-EW and $Z\gamma jj$-QCD evaluated:
    - optimization of the phase-space selection
    - contribution with an uncertainty of 3%
- Differential cross section measured for 1^{st} time
  - even though with partial statistics this will pave the way for the full Run II analysis.

Prospects:

- With an increase of the luminosity 4 times with full RunII data
  $\Rightarrow$ the statistical uncertainty will decrease on half
  $\Rightarrow$ the theory uncertainty becomes relevant

Back-up

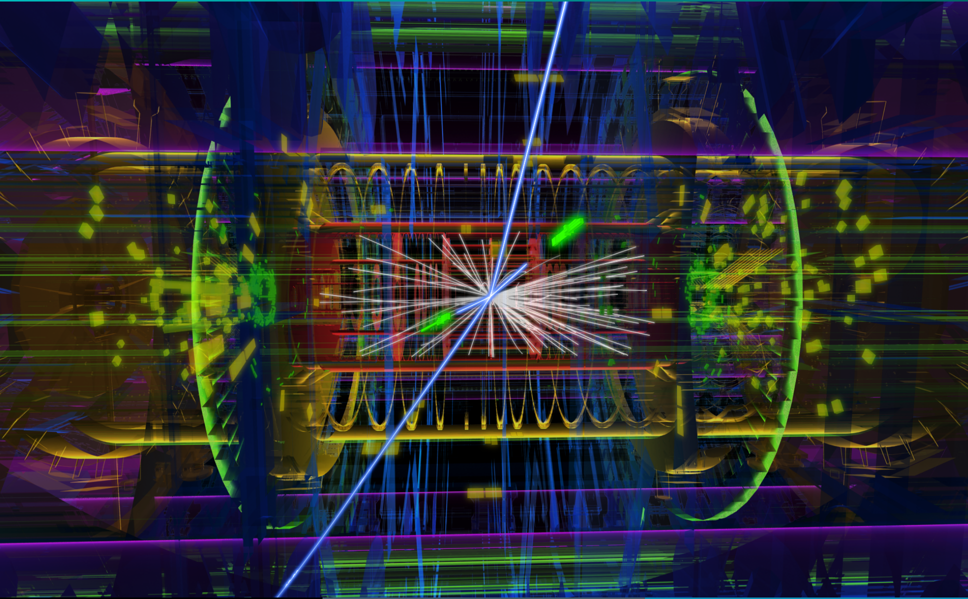

Anomalous quartic gauge couplings (aQGCs)

Any deviation from the SM predictions $\rightarrow$ a hint for new physics BSM.

- New physics could modify couplings between bosons leading to anomalous triplet and quartic gauge couplings

- presence of aQGCs enhances EW cross-section and it's more pronounced at high-energy tails.
  - $\Rightarrow$ examine variables that carry the energy of the system: transverse momentum or mass

For their description $\Rightarrow$ Effective Field Theory (EFT) with higher order dimension operators.

$$\mathcal{L}_{EFT} = \mathcal{L}_{SM} + \sum_i \frac{c_i^{(6)}}{\Lambda^2}\mathcal{O}_i^{(6)} + \sum_i \frac{f_j^{(8)}}{\Lambda^4}\mathcal{O}_j^{(8)}$$

- New interactions are suppressed by the scale of new physics Λ.
- Lowest order pure aQGCs arise from dimension-8 operators

Anomalous quartic gauge couplings (aQGCs)

Anomalous quartic electroweak gauge coupling parameters of the dimension-8 operators. Checkmark (✓) indicate a dependence of the final state on the corresponding parameter.

$VVjj$ final state	ZZ	$Z\gamma$ $\gamma\gamma$	W^+W^- WZ	$W^\pm W^\pm$	$W\gamma$	
VVV final state	ZZZ	$ZZ\gamma$ $Z\gamma\gamma$	WWZ WZZ	WWW	$WV\gamma$	$\gamma\gamma\gamma$
$f_{S,0}, f_{S,1}$	✓	–	✓	✓	–	–
$f_{M,0}, f_{M,1}, f_{M,6}, f_{M,7}$	✓	✓	✓	✓	✓	–
$f_{M,2}, f_{M,3}, f_{M,4}, f_{M,5}$	✓	✓	✓	–	✓	–
$f_{T,0}, f_{T,1}, f_{T,2}$	✓	✓	✓	✓	✓	✓
$f_{T,5}, f_{T,6}, f_{T,7}$	✓	✓	✓	–	✓	✓
$f_{T,8}, f_{T,9}$	✓	✓	–	–	–	✓

Calorimeters

Basics:

- particles to be measured are fully absorbed and their energy transformed into a measurable quantity.
- particles' interactions with the detector produces a shower of secondary particles with progressively degraded energy.

1^{st} categorization

- **Electromagnetic**: measure the energy of electrons and photons through their electromagnetic interactions.
- **Hadronic**: measure hadrons through their electromagnetic and strong interactions.

2^{nd} categorization

- **Sampling calorimeters**: a dense material for energy degradation and an active material to provide the detectable signal.
- **Homogeneous calorimeters**: one type of material for energy degradation and signal generation.

ATLAS LAr Calorimeter

active material: Liquid Argon absorber: lead

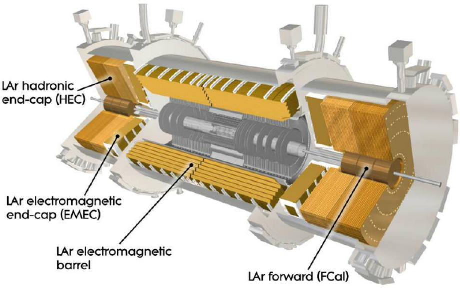

- Interactions mainly in lead absorber
- charged particles ionize Ar atoms
- electrons drift in the LAr gap where an electric field is applied
- induced signal have a characteristic triangular shape current peak $\propto$ energy lost by particles

Quantities used in the electron identification

Type	Description	Name	Rejects LF	Rejects γ	Rejects HF	Usage
Hadronic leakage	Ratio of E_T in the first layer of the hadronic calorimeter to E_T of the EM cluster (used over the range $\|\eta\| < 0.8$ or $\|\eta\| > 1.37$)	R_{had1}	x	x		LH
	Ratio of E_T in the hadronic calorimeter to E_T of the EM cluster (used over the range $0.8 < \|\eta\| < 1.37$)	R_{had}	x	x		LH
Third layer of EM calorimeter	Ratio of the energy in the third layer to the total energy in the EM calorimeter. This variable is only used for $E_T < 80\ GeV$, due to inefficiencies at high E_T, and is also removed from the LH for $\|\eta\| > 2.37$, where it is poorly modelled by the simulation.	f_3	x			LH
Second layer of EM calorimeter	Lateral shower width, $\sqrt{(\Sigma E_i\eta_i^2)/(\Sigma E_i) - ((\Sigma E_i\eta_i)/(\Sigma E_i))^2}$, where E_i is the energy and η_i is the pseudorapidity of cell i and the sum is calculated within a window of 3×5 cells	$w_{\eta 2}$	x	x		LH
	Ratio of the energy in 3×3 cells over the energy in 3×7 cells centred at the electron cluster position	R_ϕ	x	x		LH
	Ratio of the energy in 3×7 cells over the energy in 7×7 cells centred at the electron cluster position	R_η	x	x	x	LH
First layer of EM calorimeter	Shower width, $\sqrt{(\Sigma E_i(i - i_{max})^2)/(\Sigma E_i)}$, where i runs over all strips in a window of $\Delta\eta \times \Delta\phi \approx 0.0625 \times 0.2$, corresponding typically to 20 strips in η, and i_{max} is the index of the highest-energy strip, used for $E_T > 150$ GeV only	w_{stot}	x	x	x	C
	Ratio of the energy difference between the maximum energy deposit and the energy deposit in a secondary maximum in the cluster to the sum of these energies	E_{ratio}	x	x		LH
	Ratio of the energy in the first layer to the total energy in the EM calorimeter	f_1	x			LH
Track conditions	Number of hits in the innermost pixel layer	n_{Blayer}		x		C
	Number of hits in the pixel detector	n_{Pixel}		x		C
	Total number of hits in the pixel and SCT detectors	n_{Si}		x		C
	Transverse impact parameter relative to the beam-line	d_0		x	x	LH
	Significance of transverse impact parameter defined as the ratio of d_0 to its uncertainty	—$d_0/\sigma(d_0)$—		x	x	LH
	Momentum lost by the track between the perigee and the last measurement point divided by the momentum at perigee	$\Delta p/p$	x			LH
TRT	Likelihood probability based on transition radiation in the TRT	eProbabilityHT	x			LH
Track–cluster matching	$\Delta\eta$ between the cluster position in the first layer and the extrapolated track	$\Delta\eta_1$	x	x		LH
	$\Delta\phi$ between the cluster position in the second layer of the EM calorimeter and the momentum-rescaled track, extrapolated from the perigee, times the charge q	$\Delta\phi_{res}$	x	x		LH
	Ratio of the cluster energy to the track momentum, used for $E_T > 150$ GeV only	E/p	x	x		C

Electron identification - Likelihood method

Likelihood functions are constructed as the product of n pdfs for signal & background:

$$\mathcal{L}_{S(B)}(\vec{x}) = \prod_{i=1}^{n} P_{S(B),i}(x_i)$$

The signal & bkg likelihood are then combined into a discriminant $d_{\mathcal{L}}$ on which selected criteria are applied:

$$d_{\mathcal{L}} = \frac{\mathcal{L}_S}{\mathcal{L}_S + \mathcal{L}_B}$$

- Signal peaks at 1 & Background peaks at 0
- $\Rightarrow$ inconvenient since will require extremely fine binning

$\Rightarrow$ an inverse sigmoid function is used:

$$d'_{\mathcal{L}} = -\tau^{-1} ln({d_{\mathcal{L}}}^{-1} - 1)$$

The 3 working points have different threshold of this value to separate signal from background.

The measured LH identification efficiencies.

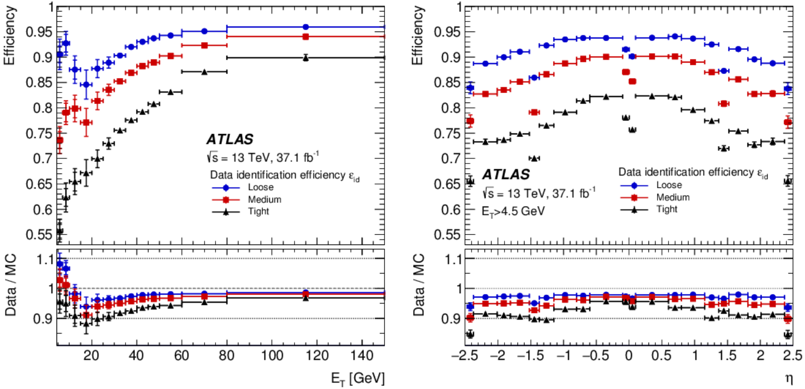

Electron isolation

Calorimeter based isolation:
a cone of size ΔR is build around the direction of candidate electron.

$$E_T^{cone,\Delta R} = \left(\sum_{i \in \Delta R} E_{T,\text{topocluster}} \right) - E_T$$

- The energies of all topological clusters, whose barycenters fall within a cone of radius ΔR are summed.
- The core energy E_T, is subtracted by removing the cells around the direction of the candidate.

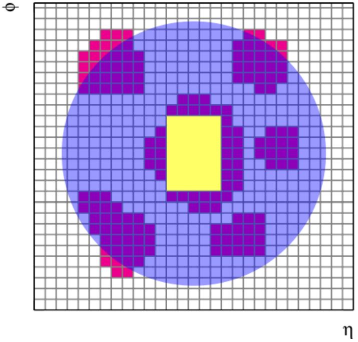

Isolation efficiencies.

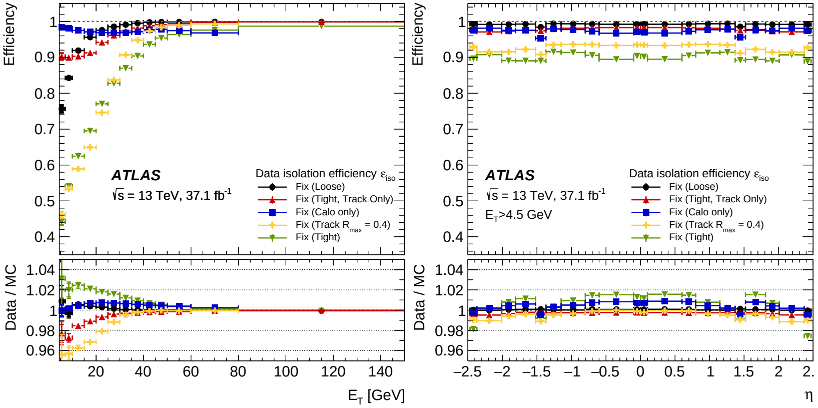

Electron identification - ZIso method

Distributions of the probe isolation for the bin:
$20\ \text{GeV} < E_T < 25\ \text{GeV}$ and $0.6 < \eta < 0.8$.

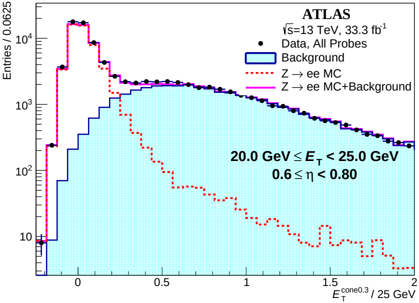

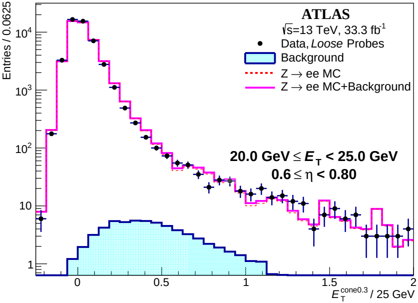

Electron identification - ZIso method

Events included in the GRL
Events pass single electron triggers
Number of vertices ≥ 1
≥ 2 tracks assigned to the vertex
Object quality criteria on ECAL cluster of the tag and probe
≥ 2 electrons in the event
Reject probe electrons within $\Delta R < 0.4$ to jet with $E_T^{\text{jet}} > 20$ GeV
For MC events: successful truth matching for tag and probe electrons

Tag electron	**Probe electron**	**Tag-Probe pair**
$E_T > 27$ GeV	$E_T \geq 15$ GeV	
$-2.47 \geq \eta \leq 2.47$ excluding $1.37 \geq \eta \leq 1.52$	$-2.47 \geq \eta \leq 2.47$	$75 \leq m_{ee} \leq 105$ GeV opposite charge pairs
match to trigger	–	
pass *Tight* ID	–	

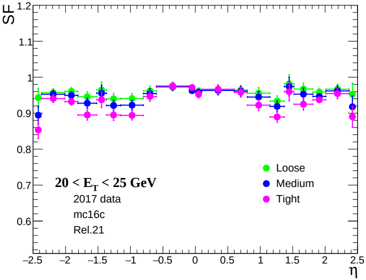

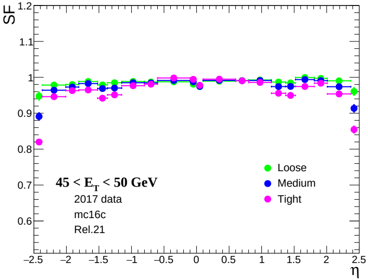

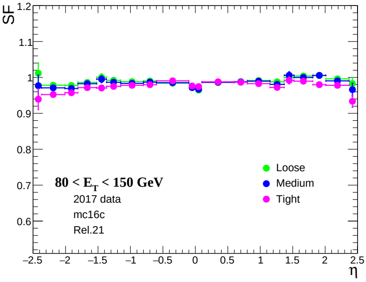

Comparison Zmass and ZIso methods

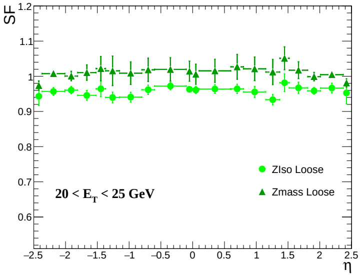

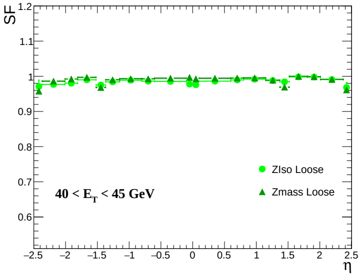

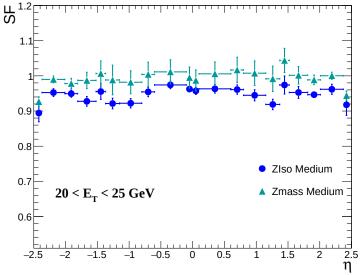

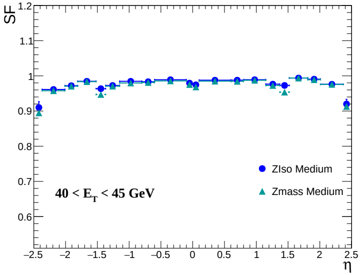

Impact of the variation of relevant parameters of the ZIso method on the scale factors

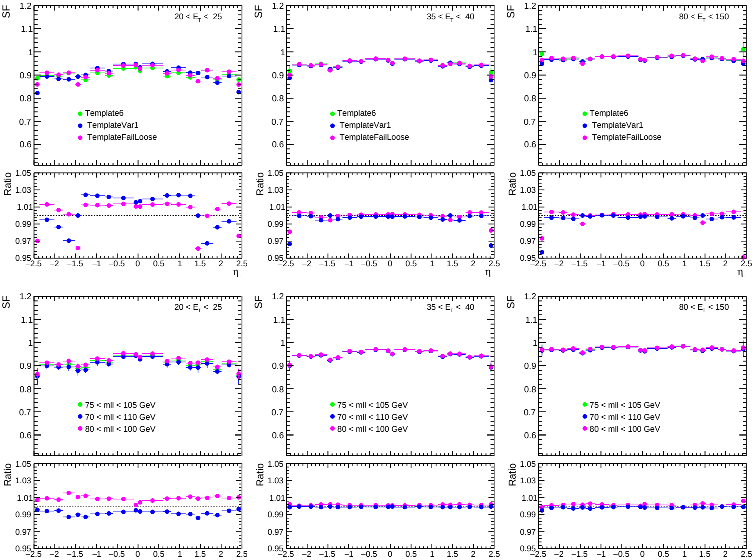

Effect of variations

2015 data:

E_T (GeV)	Template	Mass window	E_T^{cone} threshold	$E_T^{cone,\Delta R=0.4}$	Tag isolation
15-20	±5%	±2%	±0.4%	±0.4%	±0.6%
20-25	±3%	±1%	±0.4%	±0.4%	±0.5%
45-50	±0.5%	±0.1%	±0.2%	±0.3%	±0.2%
80-150	±0.3%	±0.1%	±0.2%	±0.2%	±0.1%

2016 data:

E_T (GeV)	Template	Mass window	E_T^{cone} threshold	$E_T^{cone,\Delta R=0.4}$	Tag isolation
15-20	±3%	±2%	±0.4%	±0.6%	±0.6%
20-25	±3%	±1%	±0.3%	±0.4%	±0.4%
45-50	±0.5%	±0.1%	±0.1%	±0.1%	±0.1%
80-150	±0.3%	±0.1%	±0.1%	±0.1%	±0.1%

Event pre-selection

Events included in the GRL
Events pass the single electron trigger
number of vertices ≥ 1
≥ 2 tracks assigned to the vertex
Object quality criteria on ECAL cluster of tag and probe
≥ 2 electrons in the event
≥ 1 photons in the event
Reject probe electrons within $\Delta R < 0.4$ to ANTIKT4 jet with $E_T^{\text{jet}} > 20$ GeV

Tag electron	**Probe electron**	**Photon**
$E_T \geq 25$ GeV	$E_T \geq 10$ GeV	$E_T \geq 10$ GeV
$-2.47 \geq \eta \leq 2.47$ excluding $1.37 \geq \eta \leq 1.52$	$-2.47 \geq \eta \leq 2.47$	$-2.37 \geq \eta \leq 2.37$
match to trigger	–	converted & non-converted with two tracks
pass *Tight* ID	–	pass *Tight* ID & isolated (FixedCutTight)

Tag and probe have opposite charge
$40 < M_{ee} < 90$ GeV
$M_{\text{tag-}\gamma} < 80$ GeV
$\Delta R_{\text{tag-}\gamma} > 0.4$
$\Delta R_{\text{probe-}\gamma} > 0.2$
$E_{Tprobe} + E_{T\gamma} > 30$ GeV

Event selection

Selection Cut	MC Number of events	MC %
$40 < M_{ee} < 90$ GeV	76241	100%
$M_{\text{tag-}\gamma} < 80$ GeV	70595	93%
$\Delta R_{\text{tag-}\gamma} > 0.4$	70298	99.6%
$\Delta R_{\text{probe-}\gamma} > 0.2$	70298	100%
$E_{Tprobe} + E_{T\gamma} > 30$ GeV	67085	95%

Cutflow

Electron Identification $Z \to ee\gamma$ method

Trigger (1.5 times more stat.):
single electron triggers were used with an E_T trigger threshold that from Run I to Run II was increased from 24 to 26 GeV

- HLT_e20_lhmedium_nod0_g35loose $\rightarrow$ at least 1 *Medium* electron with $E_T > 20$ GeV & a *Loose* identified photon with $p_T > 35$ GeV
- HLT_e24_lhmedium_nod0_g25medium at least 1 *Medium* electron with $E_T > 24$ GeV & a *Medium* identification photon with $p_T > 25$ GeV

$\Rightarrow$ E_T tag from 27 to 25 GeV

Photon isolation (1.2 times more stat.):

- *FixedCutTight* $\Rightarrow$ *FixedCutLoose*

FixedCut Working Point	Calo isolation	Track isolation
Tight	topoetcone40 < 0.022 pT + 2.45 [GeV]	ptcone20_TightTTVA_pt1000/pT < 0.05
Loose	topoetcone20 < 0.065 pT	ptcone20_TightTTVA_pt1000/pT < 0.05

Combined scale factors Zmass-$Z\gamma$

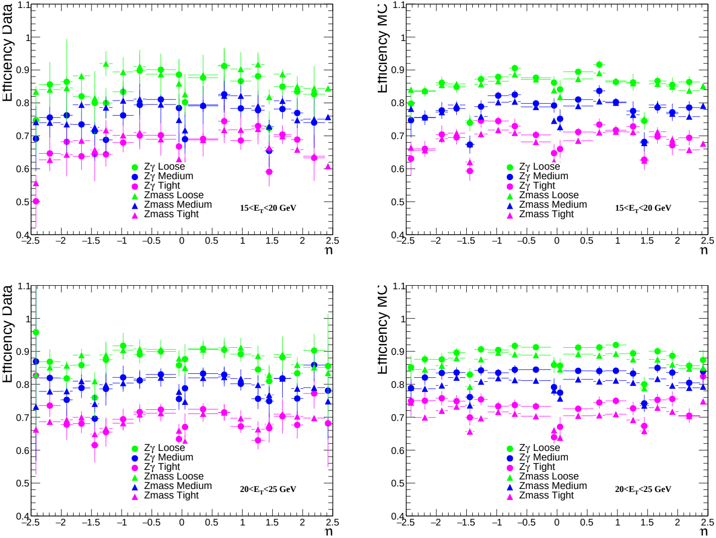

Combined scale factors ZIso-$Z\gamma$

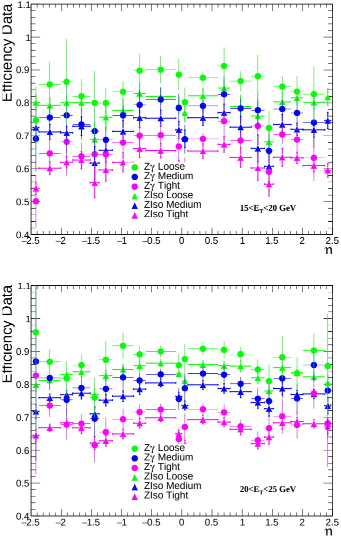

Combined scale factors Zmass-$Z\gamma$ & ZIso-$Z\gamma$

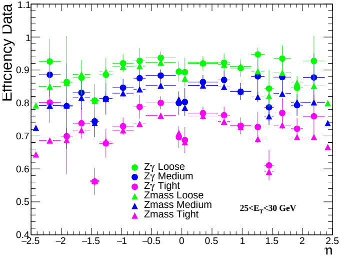

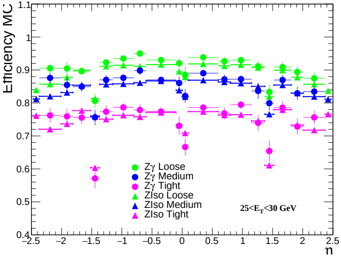

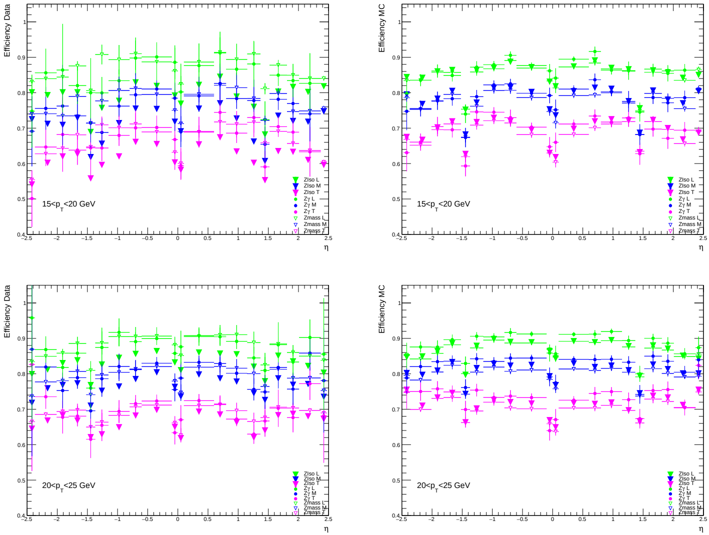
Efficiency Data
Efficiency MC
15<p_T<20 GeV
20<p_T<25 GeV
η
ZIso L
ZIso M
ZIso T
Zγ L
Zγ M
Zγ T
Zmass L
Zmass M
Zmass T

Electron SFs with $Z \to ee$ & $Z \to ee\gamma$ methods

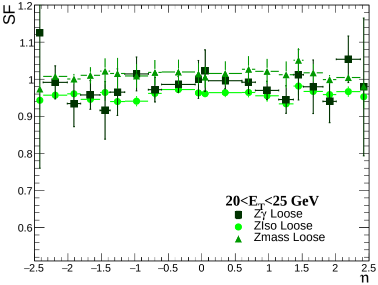

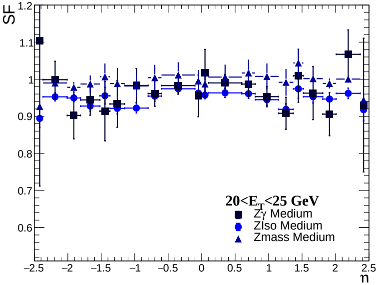

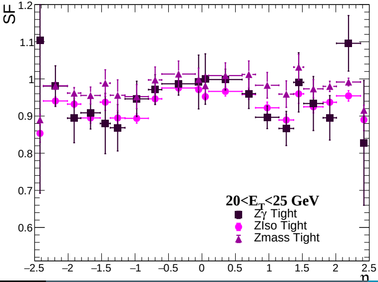

Combined scale factors $J/\psi - Z\gamma$

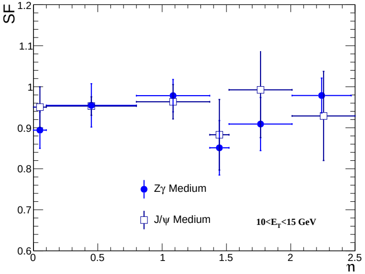

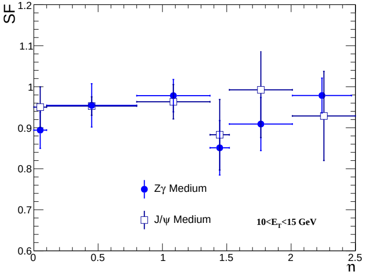

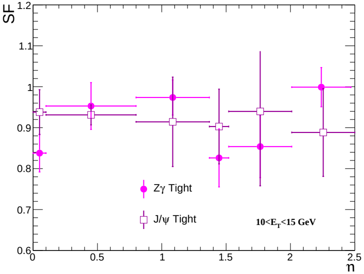

Trigger selection

Muon Channel	**Electron Channel**
Single-muon triggers:	*Single-electron triggers*:
HLT_mu20_iloose, *HLT_mu50*	*HLT_e24_lhmedium*, *HLT_e60_lhmedium*, *HLT_e120_lhloose*
di-muon trigger	*di-electron trigger*
HLT_2mu14	*HLT_2e12_lhloose*

Muon Channel	**Electron Channel**
Single-muon triggers:	*Single-electron triggers*:
HLT_mu26_ivarmedium *HLT_mu50*	*HLT_e26_lhtight_nod0_ivarloose*, *HLT_e60_lhmedium_nod0*, *HLT_e140_lhloose_nod0*
di-muon trigger	*di-electron trigger*
HLT_2mu14	*HLT_2e17_lhvloose_nod0*

Event Selection

Lepton	a pair of SFOC with $p_T^\ell > 20$ GeV $\|\eta_\ell\| < 2.47(2.5)$ for $e(\mu)$ remove e if $\Delta R(e,\mu) < 0.1$
Boson mass	$m_{\ell^+\ell^-} > 40$ GeV $m_{\ell^+\ell^-} + m_{\ell^+\ell^-\gamma} > 182$ GeV
Photon	$E_T^\gamma > 15$ GeV $\|\eta_\gamma\| < 2.37$ (excl. $1.37 < \|\eta_\gamma\| < 1.52$) remove γ if $\Delta R(\ell,\gamma) < 0.4$
Jet	$N_{jet} >= 2$, $p_T^{jet} > 30$ GeV , $\|\eta_{jet}\| < 4.5$ remove jets if $\Delta R(\ell, jet) < 0.3$ OR $\Delta R(\gamma, jet) < 0.4$ $\Delta\eta_{jj} > 1.0$
VBS baseline selection	$p_T > 50$ GeV of two tagging jets $\|\eta\| < 4.5$ of two tagging jets $m_{jj} > 150$ GeV $\zeta(Z\gamma) < 5$ $\Delta\eta_{jj} > 1$

Z+jets background estimation

Z+jets normalization ⇒ the ABCD method is used:

- data-driven
- relies on:
  - calorimeter-based isolation & photon identification criteria
- measured in a region with high statistics (low $m_{jj} < 150$ GeV).

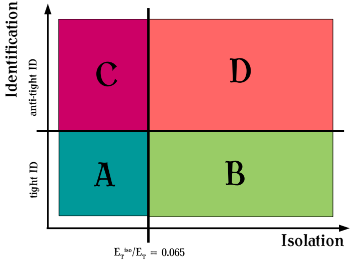

A: Signal region (tight & isolated photon):

- $N_A = N_A^{Z\gamma} + N_A^{Zjet} + N_A^{EW}$

- Extrapolation to the signal phase space:
  - data-to-MC correction factor: $f_{\text{fake}} = \frac{N^{\text{Zjet}}}{N^{Z\gamma}}$

Z+jets shape ⇒ the D region is used (after subtracting the other MC contributions)

ABCD method

The number of events N_i in each region $i = A, B, C, D$ can be expressed as:

$$\begin{aligned}
N_A &= N_A^{Z\gamma} + N_A^{Zjet} + N_A^{EW} \\
N_B &= c_B \cdot N_A^{Z\gamma} + N_B^{Zjet} + N_B^{EW} \\
N_C &= c_C \cdot N_A^{Z\gamma} + N_C^{Zjet} + N_C^{EW} \\
N_D &= c_D \cdot N_A^{Z\gamma} + N_D^{Zjet} + N_D^{EW}
\end{aligned}$$

$c_i = \frac{N_i^{Z\gamma}}{N_A^{Z\gamma}}$ are leakage coefficients

- N_i →measured directly from data
- c_i and N_i^{EW} →estimated from MC
- the expected contribution from $Z\gamma jj$-EW process is negligible

$$\begin{aligned}
N_A &= N_A^{Z\gamma} + N_A^{Zjet} + N_A^{EW} \\
N_B &= c_B \cdot N_A^{Z\gamma} + \eta_B \cdot N_A^{Zjet} + N_B^{EW} \\
N_C &= c_C \cdot N_A^{Z\gamma} + \eta_C \cdot N_A^{Zjet} + N_C^{EW} \\
N_D &= c_D \cdot N_A^{Z\gamma} + \eta_B \cdot \eta_C \cdot R_{MC} \cdot N_A^{Zjet} + N_D^{EW}
\end{aligned}$$

where $\eta_j = N_j^{Zjet}/N_A^{Zjet}$ with $j = B, C$. For the estimation of the N_D^{Zjet}:

$$N_D^{Zjet} = R_{MC} \cdot \frac{N_C^{Zjet}}{N_A^{Zjet}} \cdot N_B^{Zjet} = R_{MC} \cdot \eta_B$$

Z+jets and $Z\gamma$-QCD shapes

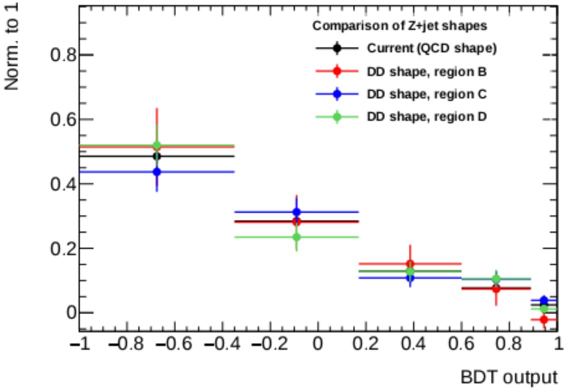

Post-unblinding checks

Since the analysis was unblinded it is also possible to run the ABCD method directly in the signal region, and compare these results with what was obtained from the fit. The prediction gives:

- $N^{fit}_{fake} = 200 \pm 15(stat + sys)$
- $N^{ABCD}_{fake} = 182 \pm 47(statonly)$

And

- $N^{fit}_{Z\gamma QCD} = 867 \pm 30(stat + sys)$
- $N^{ABCD}_{Z\gamma QCD} = 881 \pm 64(statonly)$

Both are found to be in very good agreement.

Control distributions - Inclusive region

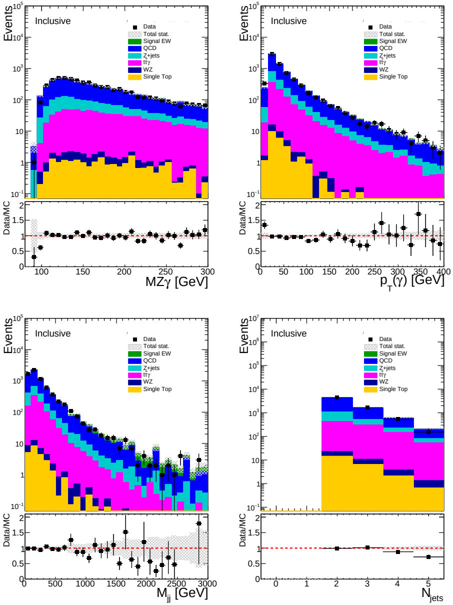

Control distributions - QCD-CR region

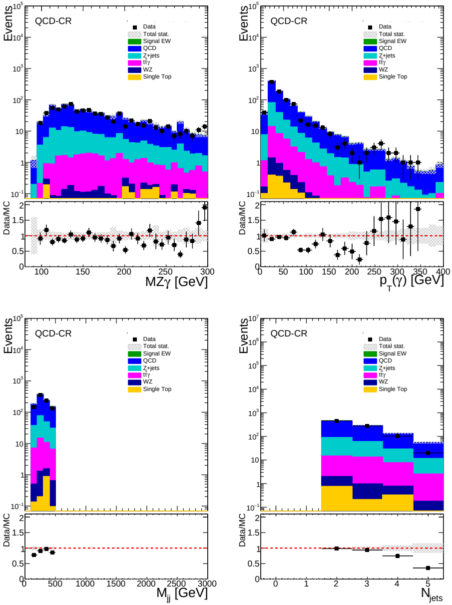

Control distributions - b-CR region

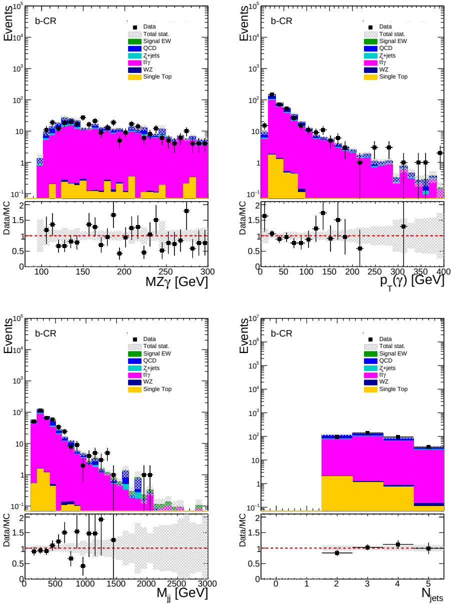

Control distributions - BDT-R region

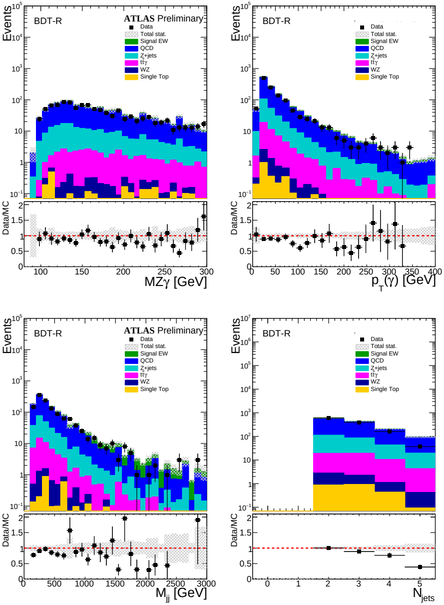

Control distributions - centrality

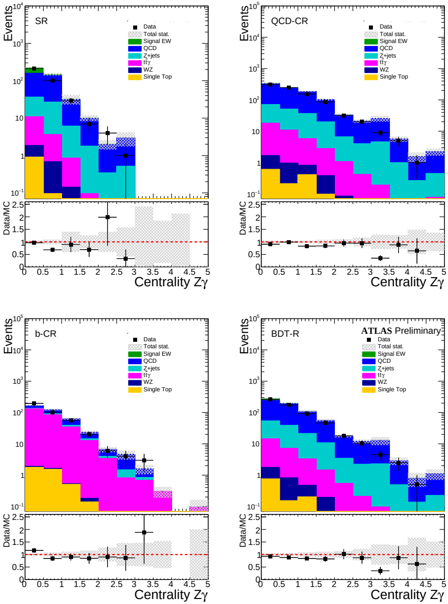

Multivariate approach

Final BDT input variables, ranked by importance for improvements in the BDT response.

Rank	Variable	Variable Importance (%)
1	$p_T(Z\gamma)$	22.3
2	Centrality	18.2
3	$m_{Z\gamma}$	18.1
4	m_{jj}	10.7
5	$min\Delta R(\gamma, j)$	5.6
6	$p_T(Z)$	4.7
7	$p_T(j_1)$	4.0
8	$\Delta\eta(j1, j2)$	3.7
9	$\Delta\phi(Z\gamma, jj)$	3.7
10	$\eta(j_1)$	3.1
11	m_Z	3.1
12	$p_T(l_1)$	2.3
13	$\Delta R(Z\gamma, jj)$	0.3

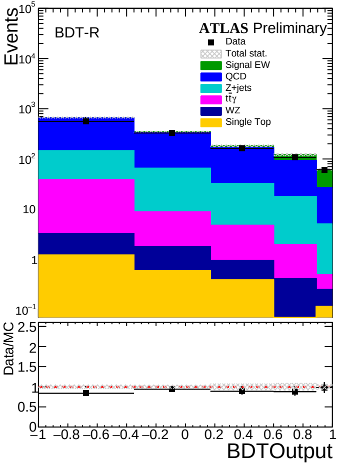

Multivariate approach & Fit procedure

Multivariate approach → gives as an output a BDT score distribution.

→ signal-like or background-like output

→ used in the fit to extract the signal strength.

Signal strength:

$\mu_{\text{EW}} = N^{\text{EW}}_{\text{meas}} / N^{\text{EW}}_{\text{exp}}$

Systematic Group	EW	QCD	$t\bar{t}\gamma$
Jets	3.5%	8.4%	5.2%
Leptons and photons	3.3%	3.9%	2.5%
Pileup	2.7%	0.02%	3.7%
Theory	1.8%	1.1%	20.7%
Flavour tagging	0.5%	0.8%	8.8%
MC statistic	3.5%	19.1%	44.9%

- extracted with a fit to the data using BDT distributions.
- μ_{QCD} & $\mu_{t\bar{t}\gamma}$ also extracted
- binned likelihood fit
- expected results → using Asimov pseudo-data

$$\mu_{EW} = 1.00^{+0.19}_{-0.18}\,(\text{stat})^{+0.08}_{-0.10}\,(\text{MCstat})^{+0.09}_{-0.08}\,(\text{syst})^{+0.13}_{-0.10}\,(\text{theo})$$

Observed significance 4.1σ (3.8σ expected)

Interference studies

Generator level cuts applied:

Generation cuts				
Object	p_T cut	η cut	ΔR cut	invariant mass cut
jets	> 15 GeV	< 5.5		
photon	> 10 GeV	< 3.0	$\Delta R(m,k) > 0.1$	$m_{jj} > 0$ GeV
leptons	> 10 GeV	< 3.0	with $m = j, \ell, \gamma$	$m_{\ell\ell} > 40$ GeV
b-quarks	> 15 GeV	< 5.5	and $k = j, \ell$	

The resulting cross sections are:

$$\sigma_{\text{gen}}(\text{EW}) = 0.0472 \pm 0.0002 \text{ pb}$$
$$\sigma_{\text{gen}}(\text{QCD}) = 5.0505 \pm 0.0016 \text{ pb}$$
$$\sigma_{\text{gen}}(\text{INT}) = 0.0022 \pm 0.0002 \text{ pb}$$

Interference - optimization of the kinematic selection

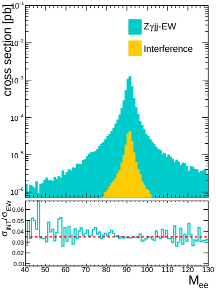

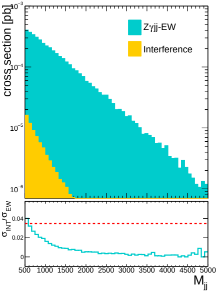

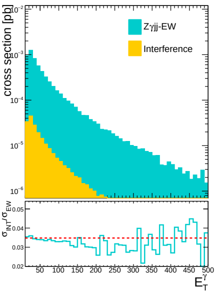

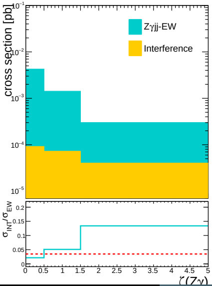

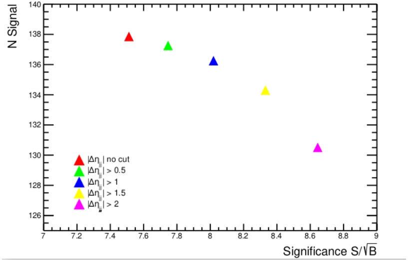

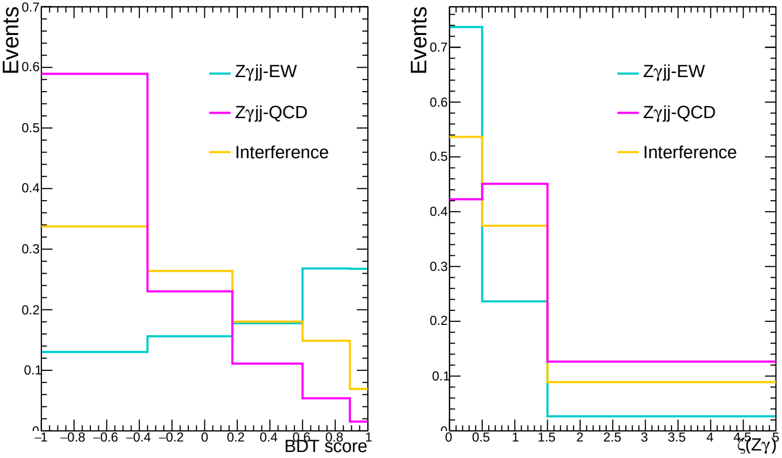
Events
Zγjj-EW
Zγjj-QCD
Interference
BDT score
ζ(Zγ)

Effect of the interference

The cross section of the 100 samples are averaged and the standard deviation is computed as:

$$\sigma_{\text{gen}} = \sqrt{\frac{\sum_i \sigma_i}{N}}, \tag{1}$$

$$\Delta\sigma_{\text{gen}} = \frac{1}{N-1}\sqrt{\sum_i (\sigma - \sigma_i)^2}. \tag{2}$$

In each corresponding phase space:

$$\sigma = \sigma_{\text{gen}} \times \frac{N_{\text{passPS}}}{N_{\text{tot}}} \tag{3}$$

with an uncertainty

$$\Delta\sigma = \sigma \times \sqrt{\left(\frac{\Delta\sigma_{\text{gen}}}{\sigma_{\text{gen}}}\right)^2 + \frac{N_{\text{passPS}}}{N_{\text{tot}}^2}\left(1 - \frac{N_{\text{passPS}}}{N_{\text{tot}}}\right)} \tag{4}$$

$$w_i = \frac{(\mathrm{EW} + \mathrm{INT})_i}{\mathrm{EW}_i}$$

where i indicates the bin number.

The resulting weights are:

BDT bin	weight
(-1,-0.35)	1.0455 ± 0.0015
(-0.35,0.17)	1.0198 ± 0.0016
(0.17,0.6)	1.0005 ± 0.0018
(0.6,0.89)	0.9873 ± 0.0022
(0.89,1)	0.9788 ± 0.0022

Centrality bin	weight
(0, 0.5)	0.9779 ± 0.0014
(0.5,1.5)	1.0122 ± 0.0014
(1.5,5)	1.0914 ± 0.0015

Interference - 3 methods for mismatch

- **Method 1** rejects the events which do not have truth values in the phase space of the measurement.
- **Method 2** uses for the re-weight the reco BDT value instead of the particle level value.
- **Method 3** applies to these events a weight = 1.

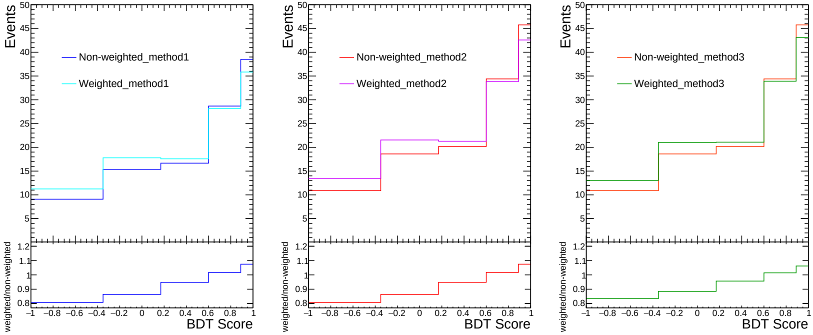

$$\sigma^{\text{fid.}}_{\text{obs. EW}} = \frac{N^{\text{EW}}_{\text{meas.}}}{N^{\text{EW}}_{\text{exp.}}} \times \sigma^{\text{fid.}}_{\text{exp. EW}} = \mu_{EW} \times \sigma^{\text{fid.}}_{\text{exp. EW}}$$

N of signal events measured in the BDT-R

$$\sigma^{\text{fid.}}_{\text{meas. EW}} = \frac{N^{\text{EW}}_{\text{meas.}}}{C \times \mathcal{L}}$$

event reconstruction efficiency:

$$C = \frac{N^{\text{EW}}_{\text{exp, reco.}}}{N^{\text{EW}}_{\text{exp, gen.}}}$$

Luminosity

$$\sigma^{\text{fid.}}_{\text{exp. EW}} = \frac{N^{\text{EW}}_{\text{exp.}}}{C \times \mathcal{L}}$$

N of simulated signal events expected in the BDT-R

Source	Uncertainty [%]
$Z\gamma jj$-EW theory modeling	$^{+9.6}_{-6.0}$
$Z\gamma jj$-QCD theory modeling	$^{+5.5}_{-6.1}$
$t\bar{t}\gamma$ theory modeling	$^{+2.2}_{-1.6}$
$Z\gamma jj$-EW and $Z\gamma jj$-QCD interference	$^{+3.2}_{-2.1}$
Jets	$^{+7.6}_{-8.2}$
Pile-up	$^{+6.4}_{-4.3}$
Electrons	$^{+0.7}_{-0.5}$
Muons	$^{+2.8}_{-2.2}$
Photons	$^{+1.2}_{-0.6}$
Electrons/photons scale	$^{+0.5}_{-0.5}$
b-tagging	$^{+1.9}_{-1.7}$
MC statistics	$^{+7.6}_{-8.2}$
Backgrounds normalization	$^{+8.9}_{-8.2}$
Luminosity	2.1
Total Systematics	$^{+27.3}_{-25.0}$

$$\sigma^{\text{fid.}}_{\text{exp. EW}} = 7.75 \pm 0.03(\text{stat}) \pm 0.2(\text{PDF}) \pm 0.4(\text{scale}) \text{ fb}$$

$$\sigma^{\text{fid.}}_{\text{obs. EW}} = 7.75^{+1.47}_{-1.39}(\text{stat.})^{+0.93}_{-0.99}(\text{exp.syst})^{+1.01}_{-0.78}(\text{mod.syst}) \pm 0.15(\text{lumi}) \text{ fb}$$

$$\sigma^{\text{fid.}}_{\text{obs. } Z\gamma jj} = 71.4 \pm 2.4\,(\text{stat.})^{+8.9}_{-6.5}\,(\text{exp.syst})^{+21.1}_{-17.0}\,(\text{mod.syst}) \pm 0.15(\text{lumi}) \text{ fb}$$

Particle level selection

Objects	Particle Level Selection
Leptons	$p_T^{\ell} > 20$ GeV and $\|\eta^{\ell}\| < 2.5$ Dressed leptons, OS charge
Photon Kinematic	$p_T^{\gamma} > 15$ GeV, $\|\eta^{\gamma}\| < 2.37$ $\Delta R(\ell,\gamma) > 0.4$
Photon Isolation	$E_T^{cone20}/E_T^{\gamma} < 0.05$
FSR cut	$M_{\ell\ell} + M_{\ell\ell\gamma} > 182$ GeV $M_{\ell\ell} > 40$ GeV
Truth Jets/Outgoing Partons (p = outgoing quarks or gluons)	At least two jets with $E_T^{jet} > 50$ GeV, $\|\eta^{jet}\| < 4.5$ $\Delta R(\ell, jet) > 0.3$ $\Delta R(\gamma, jet) > 0.4$
Search Region	$M_{jj} > 500$ GeV, $N_{bjets} = 0$
BDT Region	$M_{jj} > 150$ GeV, $N_{bjets} = 0$

Differential cross-section measurement

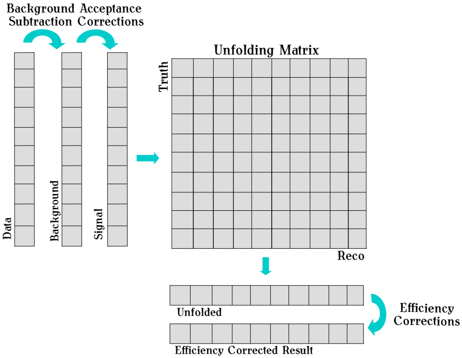

- Use of Bayesian iterative method
  - avoids the "direct attack" of finding the inverse migration matrix

Use of MC simulations
→ to construct a map that describes the migration of events (from a generated bin to a reconstructed bin).

Map = **response matrix** R (migration matrix)

$$\vec{\nu} = R \cdot \vec{\kappa} + \vec{\beta}$$

Where $\vec{\kappa}$ is the true spectra and $\vec{\nu}$ the measured one.
The true spectra can be obtained from:

$$\vec{\kappa} \equiv R^{-1} \cdot (\vec{\nu} - \vec{\beta})$$

Unfolding - treatment of Z+jets background

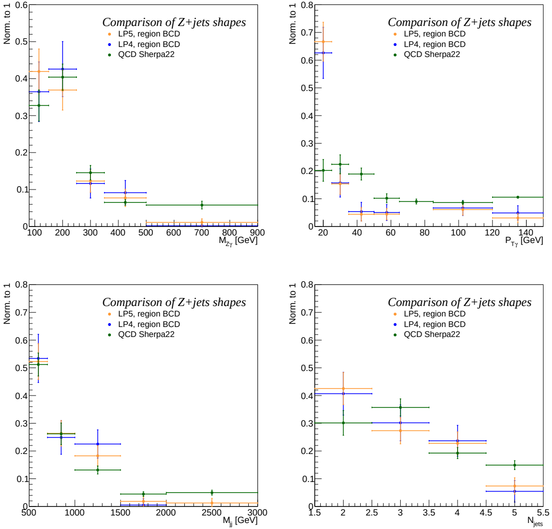

Unfolding - systematic uncertainty

Two different methods are used to calculate the uncertainty of the unfolding procedure.

- very compatible results
- the method 1 is chosen since it is use real data

	migration matrix	**Data to unfold**
Method 1	SHERPA v2.2.2 $Z\gamma jj$-QCD and EW	real data
	SHERPA v2.1 $Z\gamma jj$-QCD and MADGRAPH $Z\gamma jj$-EW	real data
Method 2	SHERPA v2.2.2 $Z\gamma jj$-QCD and EW	real data
	SHERPA v2.2.2 $Z\gamma jj$-QCD and EW	pseudo-data (SHERPA v2.1 $Z\gamma jj$-QCD and MADGRAPH $Z\gamma jj$-EW)

The background processes, namely the Z+jets, $t\bar{t}\gamma$, single top and WZ, are all scaled with an uncertainty of $\pm 20\%$

Differential cross-section measurement - results: $M_{Z\gamma}$

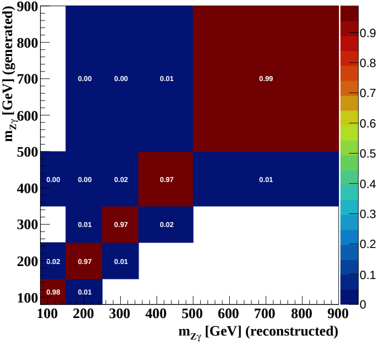

- the migration matrix is diagonal - 2 iterations
- purity: 75%-80%
- efficiency: 35%

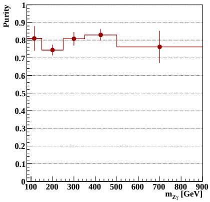

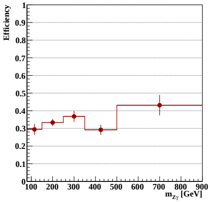

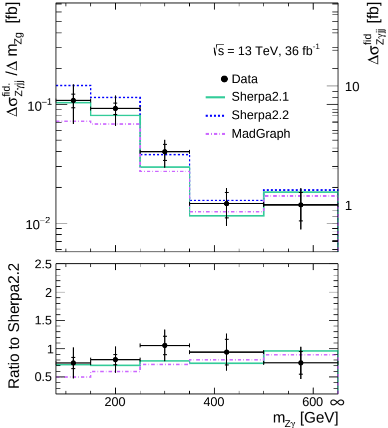

Differential cross-section measurement - results: P_T^γ

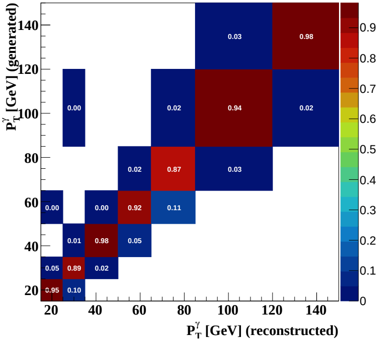

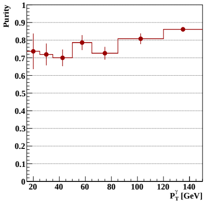

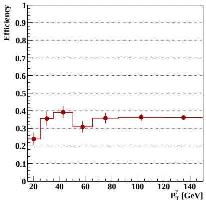

- the migration matrix is diagonal - 3 iterations
- purity: 70%-85%
- efficiency: 35%

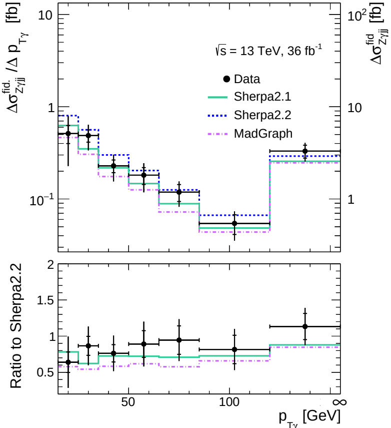

Differential cross-section measurement - results: M_{jj}

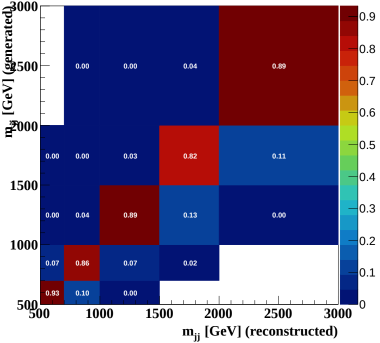

- the migration matrix is diagonal - 3 iterations
- purity: 70%-85%
- efficiency: 35%

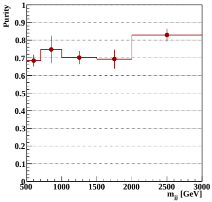

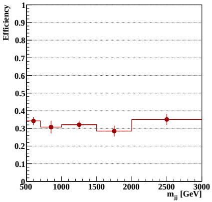

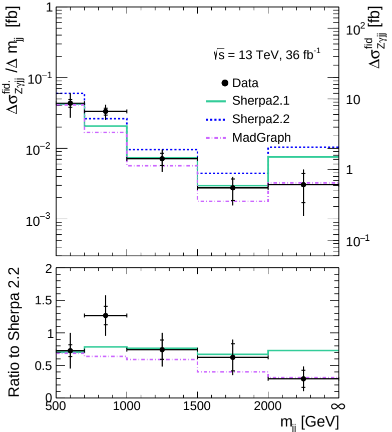

Differential cross-section measurement - systematics

$m_{Z\gamma}$ [GeV]	80 – 150	150 – 250	250 – 350	350 – 500	≥ 500
$\Delta\sigma^{\text{fid.}}_{Z\gamma jj}$ [fb]	7.55	9.23	3.99	2.19	1.00
Relative Uncertainties [%]					
Statistics	13.2	11.1	15.4	24.2	26.7
All systematics	34.2	26.4	21.5	25.0	26.8
Luminosity	2.8	2.6	2.5	2.6	2.3
Total	36.7	28.7	26.4	34.8	37.9
Uncorrelated syst.	1.0	1.2	1.4	1.7	1.3
Unfolding	0.9	0.4	0.7	1.1	0.5
Electrons	1.0	0.9	1.2	1.6	3.6
Muons	1.9	1.9	2.0	2.8	3.2
Photons	1.9	1.2	1.1	1.3	1.4
Jets	11.4	7.3	4.5	8.9	3.8
Z+jets Back.	29.0	24.3	18.3	19.7	21.9
Other Red. Back.	0.2	0.1	0.1	0.1	0.1
Irred. Background	1.0	1.2	1.4	1.7	1.3
Pileup	7.7	3.1	3.9	1.5	0.5

N_{jets}	1 – 2	2 – 3	3 – 4	≥ 4
$\Delta\sigma^{\text{fid.}}_{Z\gamma jj}$ [fb]	11.63	6.97	3.75	1.37
Relative Uncertainties [%]				
Statistics	9.9	13.5	19.1	38.0
All systematics	22.0	28.9	51.1	90.7
Luminosity	2.6	2.6	2.9	2.8
Total	24.1	31.9	54.5	98.3
Uncorrelated syst.	2.0	3.9	4.8	8.6
Unfolding	2.1	1.8	1.7	1.9
Electrons	0.8	0.8	0.9	0.8
Muons	1.9	2.0	1.7	2.9
Photons	1.2	1.6	1.8	1.3
Jets	9.2	7.7	35.0	66.7
Z+jets Back.	16.7	26.1	34.3	57.2
Other Red. Back.	0.1	0.2	0.1	0.3
Irred. Background	2.0	3.9	4.8	8.6
Pileup	5.0	3.3	5.4	9.6

Differential cross-section measurement - systematics

m_{jj} [GeV]	500 – 700	700 – 1000	1000 – 1500	1500 – 2000	$\geq$ 2000
$\Delta\sigma^{\text{fid.}}_{Z\gamma jj}$ [fb]	8.71	9.99	3.56	1.38	0.61
Relative Uncertainties [%]					
Statistics	12.4	11.2	19.9	33.4	44.5
All systematics	35.6	21.7	28.6	27.9	46.1
Luminosity	2.8	2.4	2.8	2.4	2.4
Total	37.7	24.5	34.9	43.5	64.1
Uncorrelated syst.	4.4	1.9	3.0	5.7	5.4
Unfolding	0.5	0.9	0.9	0.3	1.0
Electrons	0.9	0.7	0.9	0.8	0.7
Muons	1.7	2.1	1.7	3.3	2.4
Photons	1.7	0.9	1.6	1.4	1.9
Jets	9.1	8.4	12.7	15.5	18.4
Z+jets Back.	32.6	16.0	22.8	18.2	37.7
Other Red. Back.	0.2	0.1	0.2	0.1	0.1
Irred. Background	4.4	1.9	3.0	5.7	5.4
Pileup	5.4	5.2	5.9	0.9	9.4

P_T^γ [GeV]	15 – 25	25 – 35	35 – 50	50 – 65	65 – 85	85 – 120	$\geq$ 120
$\Delta\sigma^{\text{fid.}}_{Z\gamma jj}$ [fb]	5.12	4.87	3.43	2.72	2.37	1.90	3.30
Relative Uncertainties [%]							
Statistics	22.1	15.1	15.7	20.8	20.8	24.1	16.0
All systematics	51.0	27.0	28.2	27.9	22.5	25.3	16.3
Luminosity	4.1	2.4	2.3	2.4	2.2	2.5	2.3
Total	55.6	30.9	32.2	34.8	30.6	34.9	22.8
Uncorrelated syst.	3.8	2.5	3.8	2.8	3.5	3.0	3.6
Unfolding	0.9	0.4	0.7	0.8	0.9	0.1	0.2
Electrons	1.4	1.1	2.0	3.5	6.1	0.9	1.3
Muons	2.4	1.7	2.1	1.7	1.5	1.8	1.9
Photons	3.6	1.0	1.0	0.9	0.7	0.7	1.3
Jets	12.1	7.5	11.3	10.6	6.4	7.7	3.5
Z+jets Back.	43.4	22.2	23.0	20.8	16.7	22.5	14.6
Other Red. Back.	0.4	0.1	0.2	0.1	0.1	0.2	0.1
Irred. Background	3.8	2.5	3.8	2.8	3.5	3.0	3.6
Pileup	11.1	2.4	3.8	8.3	6.7	1.2	1.5

Closure Test

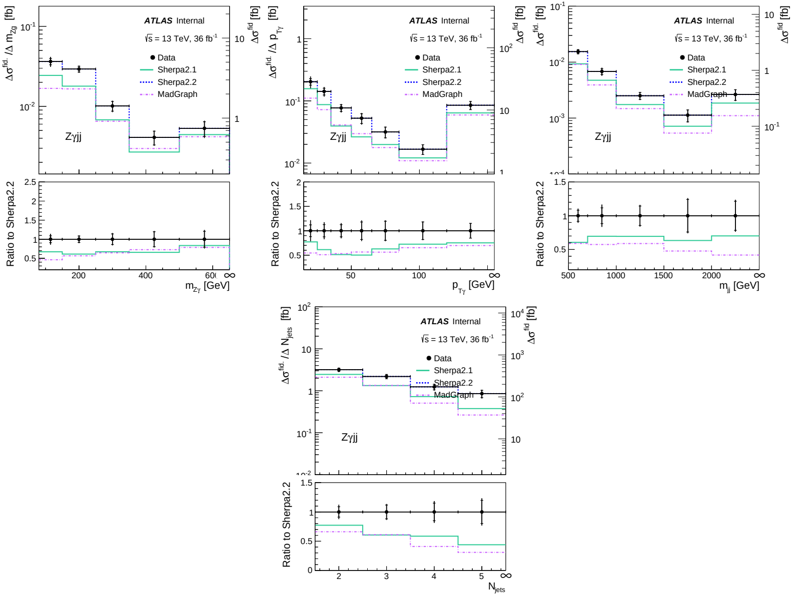

MZγ

Sample	Bin1: 80-150	Bin2: 150-250	Bin3: 250-350	Bin4: 350-500	Bin5: 500-900	Total
Data	108 $\pm$ 9.6	138 $\pm$ 8.5	63 $\pm$ 12.6	29 $\pm$ 18.6	17 $\pm$ 24	355
EW SIGNAL Mad	20.6 $\pm$ 1.4	30.4 $\pm$ 1.15	12 $\pm$ 1.7	7.2 $\pm$ 2.3	5 $\pm$ 2.7	75.3
ZgQCD Sh22	87.9 $\pm$ 12.9	108.49 $\pm$ 8.76	39.47 $\pm$ 13.43	17.5 $\pm$ 11.5	15.5 $\pm$ 18.2	268.86
Z+jets	18.46 $\pm$ 12.92	22.78 $\pm$ 8.76	8.28 $\pm$ 13.4	3.67 $\pm$ 0	3.26 $\pm$ 18.2	56.45
ttγ	2.9 $\pm$ 15.4	4.85 $\pm$ 10.8	2.79 $\pm$ 14.04	1.47 $\pm$ 18.65	0.74 $\pm$ 26.15	12.75
WZ	0.54 $\pm$ 14.2	0.73 $\pm$ 12.32	0.24 $\pm$ 18.06	0.10 $\pm$ 30.33	0.083 $\pm$ 29.51	1.69
Single Top	0.59 $\pm$ 85.02	0.212 $\pm$ 70.9	0.18 $\pm$ 70.7	0 $\pm$ 100	0 $\pm$ 100	0.98
Zγ Sh21	85.04 $\pm$ 9.89	82.24 $\pm$ 7.79	33.33 $\pm$ 9.03	20.12 $\pm$ 10.2	11.6 $\pm$ 11.3284	232
Zγ EW Sh22	21.29 $\pm$ 3.13	32.5 $\pm$ 2.52	13.4 $\pm$ 4.1	8.4 $\pm$ 5.09	6.45 $\pm$ 6.01	82.04

P_T^γ

Sample	Bin1: 15-25	Bin2: 25-35	Bin3: 35-50	Bin4: 50-65	Bin5: 65-85	Bin6: 85-120	Bin7: 120-150	Total
Data	86 ± 10.78	72 ± 11.78	54 ± 13.6	34 ± 17	32 ± 17.67	30 ± 18	47 ± 14.58	355
EW SIGNAL Mad	15 ± 1.6	12 ± 1.8	12.7 ± 1.7	8.8 ± 2.2	7.47 ± 2.38	7.52 ± 2.32	11.9 ± 1.79	75.4
ZgQCD Sh22	54.7 ± 19.29	60.2 ± 15.3	50.8 ± 11.4	27.4 ± 15.9	24.2 ± 9.7	23.2 ± 7.8	28.4 ± 4.3	269
Z+jets	11.5 ± 19.3	12.6 ± 15.3	10.67 ± 11.4	5.7 ± 15.9	5.09 ± 9.78	4.87 ± 7.87	5.95± 4.27	56.38
ttγ	2.27 ± 15.4	2.2 ± 16.9	2.54 ± 15.6	1.18 ± 21	1.4 ± 21.17	1.04 ± 20.3	2.12 ± 17	12.75
WZ	0.49 ± 15	0.24 ± 13.6	0.39 ± 16	0.14 ± 15	0.073 ± 43	0.18 ± 29	0.168 ± 25.9	1.684
Single Top	0.69 ± 74	0 ± 100	0 ± 100	0.096 ± 100	0.117 ± 100	0 ± 100	0.093 ± 100	0.996
Zγ Sh21	66. ± 12.	36. ± 11.	39.6 ± 12.	24.5 ± 13.7	24. ± 11.	16.6 *pm* 6.9	25.1269 ± 3.	231.65
Zγ EW Sh22	16. ± 3.6	12.59 ± 4.	13. ± 4.1	9.6 ± 4.5	8.3 ± 5.16	7.5 ± 4.79	14.5 ± 4.02	81.96

Mjj

Sample	Bin1: 500-700	Bin2: 700-1000	Bin3: 1000-1500	Bin4: 1500-2000	Bin5: 2000-3000	Total
Data	$149 \pm 8.$	124 ± 8.98	$55 \pm 13.$	$17 \pm 24.$	10 ± 31.6	355
EW SIGNAL Mad	16.7 ± 1.5	19.4 ± 1.4	19.2 ± 1.4	9.95 ± 1.9	$10.4 \pm 2.$	75.65
ZgQCD Sh22	137.5 ± 8.08	70.7 ± 14.8	$35. \pm 10.9$	$11.9 \pm 19.$	$13. \pm 17.7108$	268
Z+jets	28.8 ± 8.08	14.8 ± 14.8	7.4 ± 10.9	2.5 ± 0	2.8 ± 17.7	56.3
ttγ	6.4 ± 9.9	2.98 ± 12.35	1.7 ± 16.9	1.05 ± 27.5	0.63 ± 32.1764	12.76
WZ	0.65 ± 10.5	0.59 ± 13.8	0.3 ± 19.6	$0.098 \pm 47.$	$0.046 \pm 30.$	1.684
Single Top	$0.69 \pm 74.$	0.096 ± 100	0.21 ± 71.16	0 ± 100	0 ± 100	0.996
Zγ Sh21	$116. \pm 6.26$	71.6 ± 10.5	31.5 ± 10.7	6.95 ± 19.7	5.6 ± 28.2	231.65
Zγ EW Sh22	16.36 ± 3.38	18.83 ± 3.25	21.87 ± 3.15	$11. \pm 4.7$	13.9 ± 4.04463	81.96

Njets

Sample	Bin1: 1.5-2.5	Bin2: 2.5-3.5	Bin3: 3.5-4.5	Bin4: 4.5-5.5	Total
Data	155 $\pm$ 8.03	116 $\pm$ 9.28	59 $\pm$ 13	25 $\pm$ 20	355
EW SIGNAL Mad	40.76 $\pm$ 0.99	23.8 $\pm$ 1.30	8.06 $\pm$ 2.20	3.05 $\pm$ 3.58	75.67
ZgQCD Sh22	80.9 $\pm$ 14.76	96.28 $\pm$ 8.63	51.7 $\pm$ 10.37	40. $\pm$ 10.8	268.88
Z+jets	16.99 $\pm$ 14.76	20.22 $\pm$ 8.64	10.86$\pm$ 10.37	8.4 $\pm$ 0	56.47
ttγ	3.65 $\pm$ 12.97	4.70 $\pm$ 10.84	2.58 $\pm$ 14.67	1.85 $\pm$ 18.7	12.78
WZ	0.69 $\pm$ 15.5	0.56 $\pm$ 10.37	0.25 $\pm$ 12.9	0.19 $\pm$ 20.5	1.69
Single Top	0.096 $\pm$ 100	0.72 $\pm$ 72.9	0.099 $\pm$ 100	0.093 $\pm$ 100	0.99
Zγ Sh21	76.5 $\pm$ 7.9	81.66 $\pm$ 9.36	48. $\pm$ 9.00	26.05 $\pm$ 13.74	232.21
Zγ EW Sh22	58.5 $\pm$ 1.86	19.35 $\pm$ 3.5	3.6 $\pm$ 8.58	0.64 $\pm$ 16.56	82.09